Magnetoresistance Effect in CuAgCo Alloy Films

M.Sc. Thesis
in
Physics Engineering
University of Gaziantep

Supervisor
Prof.Dr.Ömer. F. BAKKALOĞLU

by

Pınar CAN

August 2005

Approval of the Graduate school of Natural and Applied Science

_____

Prof.Dr.Saadettin Özyazıcı
Director

I certify that this thesis satisfies all the requirements as a thesis for the degree of Master of Science.

_____

Prof. Dr. Zihni ÖZTÜRK
Head of Department

This is to certify that we have read this thesis and that in our opinion it is fully adequate, in scope and quality, as a thesis for the degree of Master of Science.

_____

Prof.Dr.Ömer F.BAKKALOĞLU
Supervisor

Examining Committee Members

Prof. Dr. Ömer F. BAKKALOĞLU _____

Assist.Prof. Dr. Mustafa ÖZTAŞ _____

Assist.Prof.Dr. Metin BEDİR _____

TABLE OF CONTENTS

ACKNOWLEDGEMENTS

First of all I would like to thank my supervisor Prof. Dr. Ömer F. BAKKALOĞLU. I am deeply indebted to him for all his efforts and helping me to overcome all the barriers I encountered throughout this study. His advices, continuous supports, and encouragements throughout the study are gratefully acknowledged. I would like to thank him especially for his help in literature survey, organizing and planning field studies, his advices on data interpretation and statistical analysis, reports and my thesis. It was a great privilege being a student of such a knowledgeable helpful and patient supervisor.

I would also like to thank Asist.Prof.Dr. Metin BEDİR for his helps and advices during all of the studies toward this thesis.

I would like to thank my gratitude to the research assistances, especially Research Assistants Vural Emir KAFADAR, Derya (Haydargil) TUTÇU and other staff of the Department of Engineering Physics for their kind help and friendships.

I also want to thank the following people, who helped me in the completion of this thesis; my family, for supporting and encouraging me throughout three years, especially my mother Nevin; my sisters, Cansu and Özge; my brother Çağlar and his wife Zeynep; and my father M.Oğuz; my friends, Ahmet, Seçil, Yeliz and Akif.

ABSTRACT

MAGNETORESISTANCE EFFECT IN CuAgCo ALLOY FILMS

CAN Pınar

M. S. in P.E. University of Gaziantep

Supervisor: Prof. Dr. Ömer F. BAKKALOĞLU

August 2005

The electrodeposition technique was employed to grow magnetic CuAgCo systems. The deposition was performed on Al substrate using a computer controlled potensiostat/galvanostat. Three types of CuAgCo films were grown by varying i) Co content in bath, ii) the bath pH and iii) the deposition current density. Compositional analyses indicate that all our films are mainly composed of Cu and Co elements. The amount of silver component in each system was at most 1%. The amount of Ag component in any film did not increase even when Co and Cu contents in bath were varied, and the magnitude of Ag component persisted around 1% in all the films grown in this study. SEM studies show that the CuAgCo films have granular nature.

The magnitude of the MR value in our films varied between 0.3% and 1% for the films of the Co variation from 25g/l to 50g/l, between 0.5% and 0.9% for the films of the pH variation of 5.2 to 6 and between 0.3% and 0.8% for the films of the current variation between 2.5 and 4.5 mA/cm^2. In the longitudinal and transverse MR measurements generally an isotropic behavior was detected. Although the isotropic behavior mainly indicates the GMR presence, a small anisotropic magnetoresistance (AMR) component was also detected in some of the films. The presence of AMR may be attributed to the coalescence of Co grains under the certain preparation conditions: Above certain threshold limits of the amount of Co component in bath, the pH value and the deposition current density, the connection of the magnetic grains may be formed. Above the 32% Co content in the film and above the bath pH value of 5.6, a decrease in MR effect and the presence of anisotropic MR effect were

detected while below these values of the Co content and pH, the CuAgCo films show isotropic and increasing MR effect with increasing Co content and pH. An irregular variation of the MR effect was seen in the current variation films. From the MR curves it may therefore be deduced that below the 32% Co content and below the pH value of 5.6, the magnetic Co entities in our films form superparamagnetic grains whereas the Co grains may be connected to each other to form ferromagnetically coupled grains in these films with the Co content higher than 32% and in the films with the pH value higher than 5.6 which results in the creation of AMR.

In the analysis of our superparamagnetic CuAgCo films which have Co content less than 32% or were prepared with a pH value less than 5.6, the assumption of the superparamagnetic behavior of small magnetic Co grains was employed. From this analysis, the average magnitude of Co grain was obtained to be between 9 Å and 10Å. Any correlation between the surface to volume ratio of Co grains and the highest MR at 10kOe was not detected but a linear increase in the MR value at 10kOe with the increasing Co grain concentration was found in the CuAgCo films of Co and pH variations.

Keywords: Giant magnetoresistance, Electrodeposition, CuAgCo Thin Films

ÖZET

CuAgCo ALAŞIM FİLMLERİNDE MAGNETORESİSTANS ETKİSİ

CAN Pınar

Yüksek Lisans Tezi

Gaziantep Üniversitesi Fizik Mühendisliği Bölümü

Tez Danışmanı: Prof. Dr. Ömer F. BAKKALOĞLU

Ağustos 2005

Mangnetik CuAgCo sistemlerini büyütmek için, çalışmalarımızda elektrodepolama yöntemi kullanıldı. Depolama, Al malzemesi üzerine bilgisayar kontrollü potentiostat /galvanostat kullanarak yapıldı. Üç çeşit CuAgCo filmi, i)Co miktarı ii) pH değeri iii) depolama akımı değiştirilerek büyütüldü. Yapılan bileşim analizleri, bütün filmlerimizin esas olarak Cu ve Co elementlerinden oluştuğunu gösterdi. Çalışmalarımızda, her bir sistemdeki gümüş bileşen miktarının en fazla %1 olduğu gözlendi. Co ve Cu bileşen miktarları değiştirildiğinde bile, hiçbir filmde Ag bileşen miktarının yükselmediği ve bütün filmlerde %1 civarında kaldığı tespit edildi. SEM analizleri, CuAgCo filmlerinin granular yapıda olduğunu göstermiştir.

Filmlerimizdeki MR değerlerinin büyüklüğü, Co miktarının 25g/l ile 50g/l olanlarında, % 0.3 ve % 1 olarak tespit edildi; pH değişiminin 5.2 ve 6 olduğu fimlerde, %0.5 ve %0.9; ve akım değerlerinin 2.5 ve 4.5mA/cm^2 olduğu filmlerde % 0.3 ve % 0.8 olarak değiştiği gözlendi. Boylamasına ve enlemesine olan MR ölçümlerinde genellikle izotropik bir magnetorezistans (MR) davranış gözlendi. İzotropik davranış; esas olarak çok büyük magnetorezistans (GMR) oluşumunu işaret etsede, bazı filmlerde anizotropik magnetoresistance (AMR) bileşeni de gözlendi. AMR oluşumu, belirli hazırlanma şartlarında Co parçacıklarının birleşmesiyle açıklanabilir; yani banyodaki Co miktarının, pH değerinin, depolama akım yoğunluğunun belli bir eşik limiti üzerinde, magnetik parçacıklarının birbirleriyle bağlanması gerçekleşebilir. Filmde; %32 Co miktarının üzerinde ve 5.6 pH değerinin

üzerinde MR etkisinde bir düşme olduğunu ve anizotropik MR etkisinin oluştuğunu gözledik. Co ve pH'ın bu değerlerinin altında, CuAgCo filmleri, artan Co miktarı ve pH değeriyle yükselen izotropik MR etki göstermesine rağmen; akım değiştirilen filmlerde , düzensiz bir MR etki değişimi gözlenmiştir.

% 32 den fazla Co miktarı ve pH=5.6 dan yukarı olan değerlerde, Co parçacıklarının birbirine bağlanarak ferromagnetik parçacıklarının oluşumuna ve dolayısıyla AMR oluşumuna yol açmasına rağmen, Co bileşeninin %32 olan değerinin altında ve 5.6 pH değerinin altında filmlerimizde MR eğrilerinden Co parçacıklarının süperparamagnetik parçacıklar oluşturduğu belirlendi.

% 32 den az olan Co bileşimine sahip veya pH değeri 5.6'dan az olan paramagnetik filmlerimizin MR analizleri, küçük magnetik Co parçacıklarının süperparamagnetik davranış gösterdiği temelinde yapıldı. Bu analizlerden, Co parçacığının ortalama büyüklüğünün $9A^0$ ve $10A^0$ arasında olduğu tespit edildi. Co granüllerinin yüzey-hacim oranı ve 10kOe'teki en büyük MR arasında herhangi bir orantılı bağlantı tespit edilmedi, fakat Co ve pH değişimli CuAgCo filmlerinde artan Co konsantrasyonu ile 10kOe'teki MR değerinde lineer bir yükseliş görüldü.

Anahtar Kelimeler: Giant magnetorezistans,Elektrodepolama, CuAgCo Alaşım Filmleri

LIST OF FIGURES

LIST OF TABLES

LIST OF SYMBOLS

a_0	Lattice constant
Amp	Ampere
A	Area of the deposit in cm^3
A^0	Angstrom
AMR	Anisotropic magnetorezistance
B	Induction field
CVD	Chemical vapor deposition
C, T_f	Cruie constant
D	Density of the metal (gram cm^3)
dMR	Variation of magnetoresistance
dH	Variation of magnetic field
EBE	Electron beam epitaxy
EDX	Energy dispersive X-ray analysis
F	Faraday Constant
FM	Ferroemagnetic
g	Gram
GMR	Giant magnetoresistance
H	Applied magnetic field
H_c	Coercieve field
H_s	Saturation applied field
HTS	High temperature superconducting
I	Ampere

k	Kilo
K	Kelvin
K_b	Boltzman constant
L (μH/kT)	Langevin function
l	Litre
mm	Milimeter
M	Gram moles of the metal deposited
MBE	Molacular Beam Epitaxy
MOCVD	Metalorganic Chemical Vapordeposition (MOCVD)
M_r	Remanent Magnetization
M_s	Saturation Magnetization
MR	Magnetoresistance
M_w	Atomic weight
n	Mole
N_a	The number of atoms in a mole
Nm	Nanometer
NM	Non-magnetic
N_{Co}	Average number of the Co atoms in a grain
O_e	Oersted
PLD	Pulsed Laser Deposition (PLD)
R	Resistivity
Q	Coulomb
Q_e	Coulomb (electrical charge)
r_g	Radii
k	Boltzman consant

SEM	Scanning Electron Microscopy
SPM	Superparamagnetism
t	Second
T	Thickness in cm
T_N	Neel temperature
V_g	The average volume of superparamagnetic grains
V	Volume of the deposited metal in cm^3
X	Susceptibility
Z	Effective concentration
Ω	Ohm
$(\Delta\rho/\rho)_s$	Saturation value of the MR
~	Approximately
θ	The angle between the magnetization vector and the applied magnetic field

CHAPTER 1

INTRODUCTION

In recent years, one of the most interesting and widely investigated materials has been the magnetic alloy films. Superlattices, multilayers, granular alloys, nanolayers, nanowires are these kinds of materials.

Extensive research efforts are being made in this class of metallic materials as their applications in data storage industry in particular, and magnetic sensors in general are in great demand [1]. The potential applications in the magnetic recording and sensor technologies are the reasons behind the attention on these alloy films. The inhomogeneous alloy systems show peculiar magnetic and electrical properties such as magnetoresistance effect.

The giant magnetoresistance effect (GMR) is observed in the magnetic granular films and magnetic multilayer systems. The simplest of the structures, exhibiting GMR, is a granular system consisting of nanometric ferromagnetic (FM) granules embedded in a non-magnetic (NM) metallic matrix [1, 2]. Magnetic superlattices consist of ferromagnetic layers and non-ferromagnetic layers. Ferromagnetic layers are composed of Fe, Ni, Co and their binary alloys. Non-ferromagnetic layers are composed of Cu, Ag, Au, AgCu etc.

The most interesting feature of superlattices is that there has been a variation with the electrical resistance under the condition of an outer magnetic area. This is called as ‘giant magnetoresistance’. This was first invented in Fe/Cr superlattices which were done by MBE (Molecular Beam Epitaxy) method. After these, many studies were done about magnetic superlattices like Fe/Cr, Co/Cu, Co/Ag etc. (Parkin 1991, Mosca 1991, Petroff 1991, Bian 1993, Barthelemy 1999) [3].

There are many factors which affect the magnitude of GMR. It was reported that GMR of multilayers changes periodically with the thickness of non-magnetic layer [4, 5]. GMR also varies with the thickness of the ferromagnetic layer [6, 7].

The structurel, electrical, optical, and magnetic properties of thin film made them one of the essential components of all advanced electronic devices. A number

of different techniques have introduced to grow and deposite these metallic multilayers like

-Molecular Beam Epitaxy (MBE)

-Electron Beam Epitaxy (EBE)

-Sputtering

-Thermal Evaporation

-Electron Beam Evaporation

-Chemical Vapor Deposition (CVD)

-Metal organic Chemical Vapor deposition (MOCVD)

-Pulsed Laser Deposition (PLD)

The techniques such as MBE, EBE, sputtering, PLD, and MOCVD have been successfully employed for the deposition of high temperature superconducting (HTS) materials. We can show some advantages and disadvantages of different thin film growth techniques like these:

Heat source	Advantages	Disadvantages
Thermal evaporation	no radiation	contamination
Electron beam evaporation	ion contamination	radiation
Sputtering	no radiation	contamination
MBE	no contamination	ultra high vacuum
PLD	no radiation, Low contamination	expensive
Electrodeposition	cheap, room temperature, No radiation	contamination

Besides these vacuum techniques there is an alternative way for deposition of thin films. It is electrodeposition technique. More kinds of granular films can be deposited at room temperature and pressure without using vacuum systems. This technique is cheaper, simpler and it has high deposition rate.

It is possible to prepare magnetic layers which are thinner than 1nm. Electrodeposition method firstly used to product nanolayers by Blum in 1921. Blum deposited pure Cu and Ni like consecutive layers. After Blum, Brenner achieved very thin Cu/Bi layers with 300 nm thickness by using primer solution in 1963. After achieving deposition of very thin layers, the electrodeposition method is started to be used more often.

Ferromagnetic layers which are produced by electrodeposition method show much GMR characteristic. It is first shown in CoNiCu/Cu films.

GMR values are bigger in nanolayers at room temperature than conventional superlattices. So that, GMR obtained from nanolayers are more useful for producing sensors.

Electrodeposition has been used for preparation of thin and thick films of ferroelectric, piezoelectric, magnetic materials, granular alloys, superconductors, and semiconductors. The electrodeposition is especially attractive for the design of solid-oxide fuel cells, solar cells, electrohromic devices, microelectronic devices, fiber-reinforced composite, and baterries. It is an important tool in the formation of nanostructured materials [8, 9, 10].

Its advantages include the feasibility of up-scaling to large substrate areas and production volume. Moreover, the deposition equipment is relatively simple and the deposition temperature is considerably lower than in many other methods. These features make electrodeposition a low-cost deposition method. Thus the fact that the solar cell efficiencies achieved with electrodeposited film are generally somewhat lower than those achieved by the more expensive gas-phase methods is not necessarily a major drawback, since it is compensated by the lower process costs.

Electrodeposition offers rigid control of film thickness, uniformity, and deposition rate and especially attractive owing to its low equipment cost and starting materials. Due to the use of an electric field, electrodeposition is particularly suited for the formation of uniform films on substrates of complicated shape, impregnation of porous substrates, and deposition on selected areas of the substrates.

Recently, electrodeposition gained renewed attention with the adoption by major companies of a copper plating process for the fabrication of interconnects in integrated circuits [11, 12]. In this case, the electroplating technique is especially interesting due to its low cost, high throughput and high quality of the deposits and excellent via/trench filling capabilities. Several groups have also reported current-in-plane giant magnetoresistance (GMR) for electrodeposited multilayers consisting of alternating layers of a magnetic and a nonmagnetic metal deposited from a single electrolyte [13].

Nevertheless, electrodeposition has one feature that can be a major disadvantage, namely the need to use a conducting substrate. This advantage can be circumvented by employing evaporated or sputtered seed layers, i.e., very thin

metallic layers used to electrodeposit metals onto insulating or semiconducting substrates [14]. However, semiconducting substrates can conduct sufficiently well to allow electrodeposition, making the direct electrodeposition of magnetic thin films and multilayers directly on semiconductors a subject of fundamental and partial significance. Such deposition could lead to the integration of an efficient, inexpensive and convenient method for fabricating thin layers with silicon technology, for example.

CHAPTER 2

MAGNETISM AND MAGNETORESISTANCE

2.1 Theory of Magnetism:

It is an aspect of electromagnetism, one of the fundamental forces of nature. Magnetic forces are produced by the motion of charged particles such as electrons, indicating the close relationship between electricity and magnetism. The most familiar evidence of magnetism is the force observed to act between magnetic materials such as iron. More subtle effects of magnetism, however, are found in all matter. In recent times these effects have provided important clues to the atomic structure of matter.

The phenomenon of magnetism has been known of since ancient times. When a piece of iron is stroked with lodestone; the iron itself acquires the same ability to attract other pieces of iron. The magnets thus produced are polarized—that is, each has two sides or ends called north-seeking and south-seeking poles. Like poles repel one another, and unlike poles attract. The earth itself behaves like a giant magnet with its north and south poles. Experiments show that the strength of attraction and repulsion of magnets is linearly proportional to the pole strengths and inversely proportional to the distance between them.

The magnetic properties of materials are classified in a number of different ways. However most widely used classification of magnetic materials is based on how the material reacts to a magnetic field. When a magnetic material is subjected to a magnetic field it responds positively or negatively. In positive respond the applied magnetic field is increased by the magnetic material but in the negative respond it is decreased by the opposing internal magnetic field of the material. Susceptibility, χ, is the magnetic response of a material to the magnetic field and formulized as

$$\chi = \frac{M}{H} \tag{2.1}$$

where M is magnetization which is the amount of magnetic moments in unit volume, and H is the applied field. Temperature can affect the magnetic properties of a material. The temperature at which a metal loses its magnetism is called the Curie temperature, and it is different for every metal. The Curie temperature for cobalt, for example, is about 1388K. Considering their responds to the applied magnetic field i.e. their susceptibilities, magnetic materials are generally classified as i) diamagnetic ii) paramagnetic, iii) ferromagnetic, iv) ferrimagnetic, v) antiferromagnetic materials, vi) superparamagnetic etc. [15, 16, 17].

2.1.1 Diamagnetism

Diamagnetic materials, when placed in a magnetic field, have a magnetic moment induced in them that opposes the direction of the magnetic field. This property is now understood to be a result of electric currents that are induced in individual atoms and molecules. These currents, according to Ampere's law, produce magnetic moments in opposition to the applied field. Many materials are diamagnetic; the strongest ones are metallic bismuth and organic molecules, such as benzene, that have a cyclic structure, enabling the easy establishment of electric currents, plants, water, soil, wood, your skin. The susceptibility of a diamagnetic material is negative. When the field is zero, the magnetization is zero. The diamagnetic susceptibility depends on an atom’s electron content and the areas of the occupied orbital. The susceptibility is small and independent of both applied field strength and temperature. Ionic and covalent (rare-earth) crystals are diamagnetic. Diamagnetic susceptibility is observed most clearly in those solids in which the atomic shells are completely filled.

2.1.2 Paramagnetism

These are metals that are weakly attracted to magnets. They include aluminum, gold, and copper. The magnetic moments of a paramagnetic substance are randomly oriented in the absence of any magnetic field.

Paramagnetic behavior results when the applied magnetic field lines up all the existing magnetic moments of the individual atoms or molecules that make up the material. This results in an overall magnetic moment that adds to the magnetic field. Paramagnetic materials usually contain transition metals or rare-earth elements that

possess unpaired electrons. Paramagnetism in nonmetallic substances is usually characterized by temperature dependence; that is, the size of an induced magnetic moment varies inversely to the temperature. This is a result of the increasing difficulty of ordering the magnetic moments of the individual atoms along the direction of the magnetic field as the temperature is raised. Paramagnetic materials like aluminum and copper become more magnetic when they are very cold. In the presence of a field, there is a partial alignment of the atomic magnetic moments in the direction of the field, resulting in a net magnetization and positive susceptibility .The efficiency of the field in aligning the moments is opposed by the randomizing effects of temperature. This results in temperature dependent susceptibility known as the 'CURIE LAW ':

$$X=\frac{C}{T} \qquad (2.2)$$

As the temperature increases, then the thermal agitation will increase and it will become harder to align the magnetic moments, and hence the susceptibility will decrease. This is called 'LANGEVIN MODEL'. The effect of temperature is to randomize the direction of the dipole. The energy is least when the moment is parallel to the field.

2.1.3 Ferromagnetism

Strongly magnetic ferromagnetic materials like iron, cobalt and nickel lose all their magnetic properties if they are heated to a high enough temperature. The atoms become too excited by the heat to remain pointing in one direction for long. The rare-earth metals Gd, Dy and insulating transition metal oxide CrO_2 all become ferromagnetic under suitable circumstances.

A ferromagnetic substance remains a magnetic moment even when the external magnetic field is reduced to zero. This effect is a result of a strong interaction between the magnetic moments of the individual atoms or electrons in the magnetic substance that causes them to line up parallel to one another. In ordinary circumstances these ferromagnetic materials are divided into regions called domains; in each domain, the atomic moments are aligned parallel to one another. Separate domains have total moments that do not necessarily point in the same direction.

Thus, although an ordinary piece of cobalt might not have an overall magnetic moment, magnetization can be induced in it by placing the iron in a magnetic field, thereby aligning the moments of all the individual domains. The energy expended in reorienting the domains from the magnetized back to the demagnetized state manifests itself in a lag in response, known as hysteresis .Ferromagnetic materials, when it is heated, eventually lose their magnetic properties. This loss becomes complete above the Curie temperature which is discovered in 1895. (The Curie temperature of metallic iron is about 770°C/1300° F.)

Ferromagnetism appears only below a certain temperature (ferromagnetic transition temp. =Curie temp.)This temperature depends on the substance. Above this temperature the moments are oriented randomly, resulting in a zero net magnetization. In this region the substance is paramagnetic. (We can convert all ferromagnets to paramagnets but we cannot convert all paramagnets to ferromagnets.)

$$X=\frac{C}{T-T_f} \tag{2.3}$$

C: Curie constant, T_f : Curie temperature. In the temperature range $T<T_f$ spontaneous magnetization is referred to as 'saturation magnetization'. This magnetization increases as the temperature is lowered. Ferromagnetism appears in both metals and insulators.

2.1.4 Ferrimagnetism

The main ferrimagnetic material is magnetite, a crystal which occurs naturally in rocks called lodestones, which were the first magnetic materials discovered by man. The crystal structure of the mineral allows only some of the atoms to line up when a magnetic field is present, so it is only weakly attracted to a magnet. The crystal itself is only a weak magnet. However, if magnetite is ground up into a powder, its magnetic properties, although weak, are very useful. Magnetite powder is what coats the tape in a cassette, allowing you to record sound and music. Magnetite powder mixed with plastic and pressed into rectangles makes the stick-on magnets used for fridge magnets.

2.1.5 Antiferromagnetism

The dipoles have equal moments, but adjacent dipoles point in opposite directions. Thus the moments balance each other, resulting in no domain formation and a zero net magnetization. Antiferromagnetism is exhibited by many compounds involving transition metals. It also disappears at a certain point as the temperature raised. The transition point is called Neel temp. T_N. Above this point the substance is paramagnetic, and

$$\chi = \frac{C}{T + T_N} \tag{2.4}$$

2.1.6 Superparamagnetism and Superparamagnetic materials:

Normally, coupling forces in ferromagnetic materials cause the magnetic moments of neighboring atoms to align, resulting in very large internal magnetic fields. At temperatures above the Curie temperature (or the Neel temperature for antiferromagnetic materials), the thermal energy is sufficient to overcome the coupling forces, causing the atomic magnetic moments to fluctuate randomly. Because there is no longer any magnetic order, the internal magnetic field no longer exists and the material exhibits paramagnetic behavior. The energy required to change the direction of magnetization of a crystallite is called the Crystalline anisotropy energy and depends both on the material properties and the crystallite size. As the crystallite size decreases, so does the Crystalline anisotropy energy, resulting in a decrease in the temperature at which the material becomes superparamagnetic. In the granular type of magnetic systems, there may be three types of magnetic structures [18]. The first is the multi domain structure which is larger than a size called 'critical size'. In this type magnetization process takes place through the domain wall displacement and therefore its coercive field is generally small. The second is a single domain structure found below the critical size. Here the magnetization process is due to the rotation of the magnetization vector and hence a large coercive force is expected with large anisotropy energy. The third type refers to the superparamagnetic particles. Superparamagnetism occurs when the material is composed of very small crystallites (1-10nm). In this case even though the temperature is below the Curie or Neel temperature and the thermal energy is not sufficient to overcome the coupling forces between neighboring atoms, the thermal

energy is sufficient to change the direction of magnetization of the entire crystallite. The resulting fluctuations in the direction of magnetization cause the magnetic field to average zero. The material behaves in a manner similar to paramagnetism, except that instead of each individual atom being independently influenced by an external magnetic field, the magnetic moment of the entire crystallite tends to align with the magnetic field. The coercive force is decreased by the thermal excitation.

However, requires a time dependence on the size of the particle. Their magnetic susceptibility is between that of ferromagnetic and paramagnetic materials [19]. We can see the effect of magnetic field on some magnetic materials in figure 2.1.

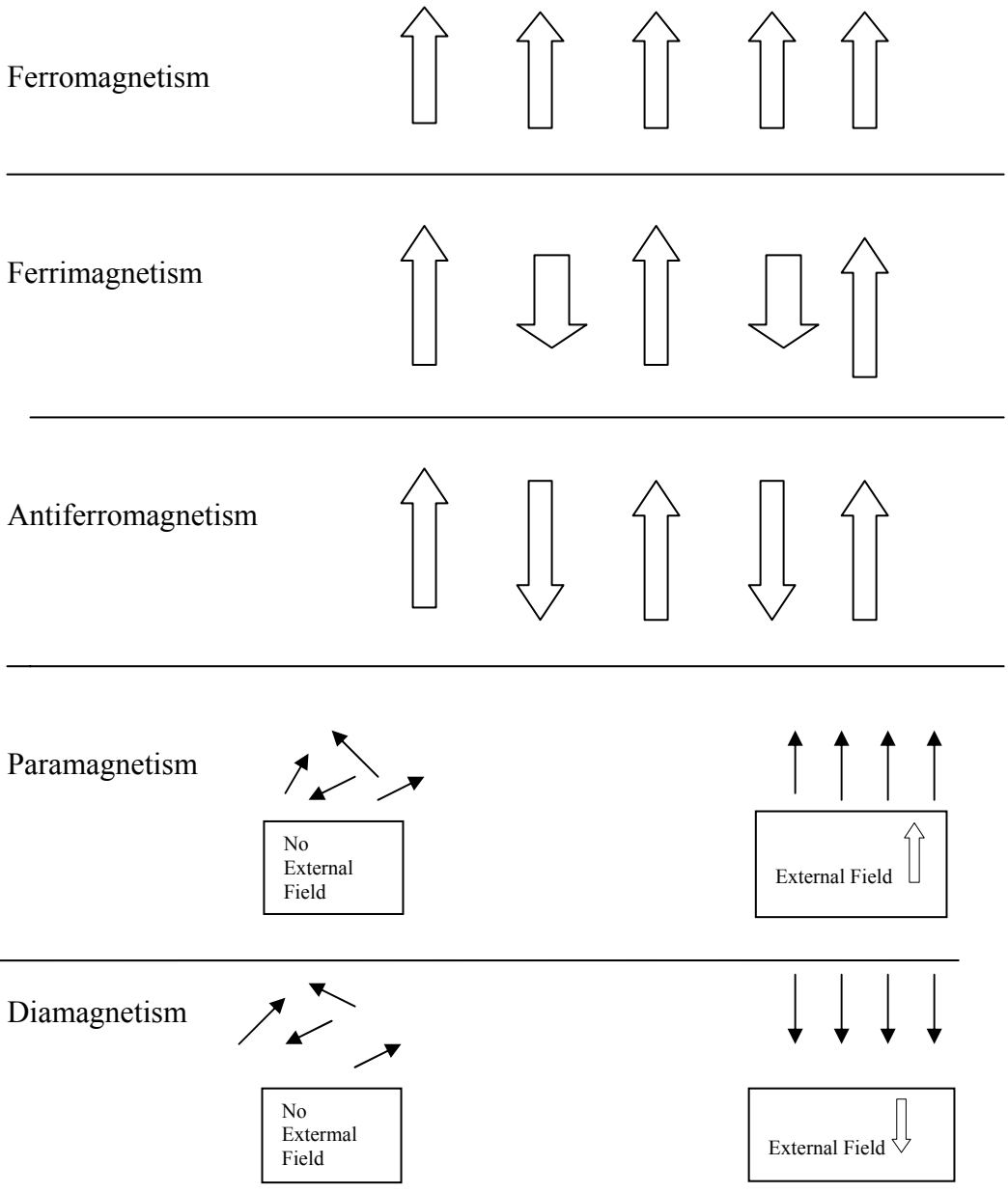

Figure 2.1 Alignments of the atomic magnetic moments

2.2 Magnetic Hysteresis Loop

The Hysteresis-loop is a result of the variation of the applied field H. The hysteresis loop describes the orientation of the material throughout a change in magnetic field intensity. The nature of material is to accept the magnetic field by aligning the material to the surrounding field. The magnetic field is then changed which is detected by the material. However, the nature of the material is to resist change which describes the slow movement towards the other magnetic pole.

The hysteresis loop for a magnetic and ferrimagnetic material can be obtained by measuring the intensity of magnetization M or the induction field B as a function of the applied field H. The hysteresis loop corresponds to the magnetization of a ferromagnetic sample which is initially unmagnetized. At normal conditions, the magnetic moments of a ferromagnetic material are aligned parallel to each other only over a microscopic space or region called domains. The total magnetization of the domains is zero because their moments are randomly aligned relative to each other. All domains are aligned randomly and the total magnetization of the sample is zero. When the ferromagnetic sample is placed in a magnetic field (H), the domains will start to align their moments in the direction of the magnetic field. The loop is generated by measuring the magnetic flux **B** of a ferromagnetic material while the magnetizing force **H** is changed. A ferromagnetic material that has never been previously magnetized or has been thoroughly demagnetized will follow the dashed line as **H** is increased. As the line demonstrates, the greater the amount of current applied **(H+)**, the stronger the magnetic field in the component **(B+)**. At point "a" almost all of the magnetic domains are aligned and an additional increase in the magnetizing force will produce very little increase in magnetic flux. The material has reached the point of magnetic saturation. When **H** is reduced back down to zero, the curve will move from point "a" to point "b." At this point, it can be seen that some magnetic flux remains in the material even though the magnetizing force is zero. This is referred to as the point of remainment on the graph and indicates the remanence or level of residual magnetism in the material. (Some of the magnetic domains remain aligned but some have lost there alignment.) As the magnetizing force is reversed, the curve moves to point "c", where the flux has been reduced to zero. This is called the point of coercivity on the curve. (The reversed magnetizing force has flipped enough of the domains so that the net flux within the material is

zero.) The force required to remove the residual magnetism from the material, is called the coercive force or coercivity of the material. As the magnetizing force is increased in the negative direction, the material will again become magnetically saturated but in the opposite direction (point "d"). Reducing **H** to zero brings the curve to point "e." It will have a level of residual magnetism equal to that achieved in the other direction. Increasing **H** back in the positive direction will return **B** to zero. Notice that the curve did not return to the origin of the graph because some force is required to remove the residual magnetism. The curve will take a different path from point "f" back the saturation point where it with complete the loop.

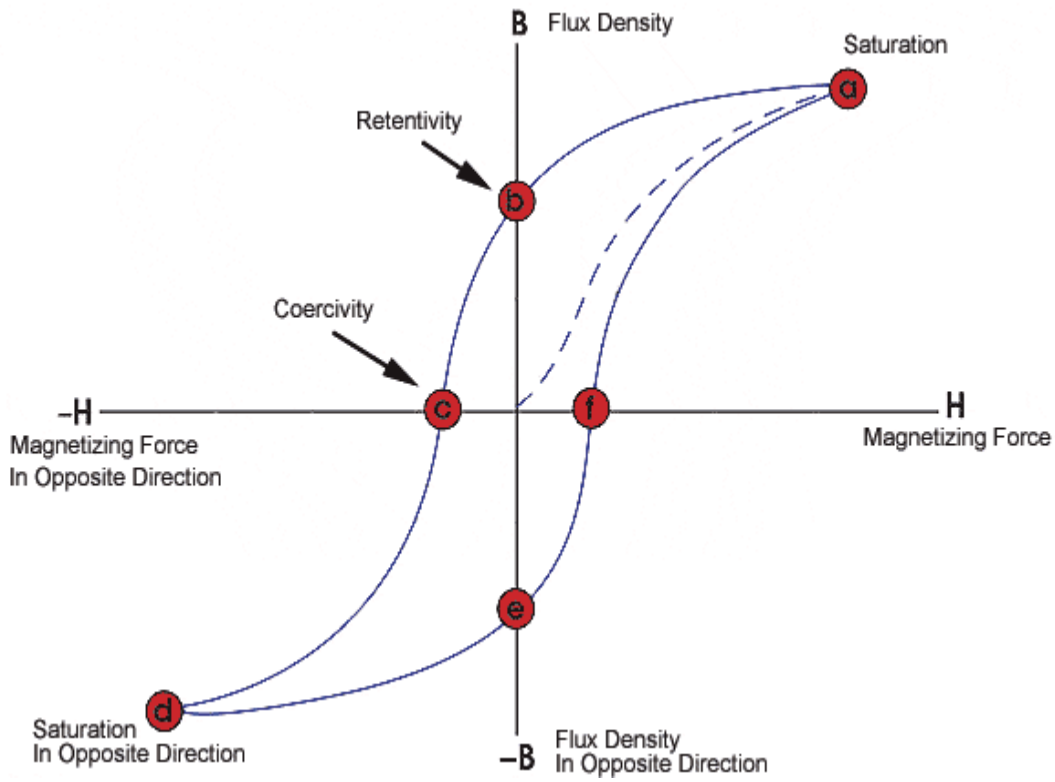

Figure2. 2. Hysteresis Loop

2.3 Applications of Magnetism

Numerous applications of magnetism and of magnetic materials have arisen in the past 100 years. The electromagnet, for example, is the basis of the electric motor and the transformer. In more recent times, the development of new magnetic

materials has also been important in the computer revolution. Computer memories can be fabricated using bubble domains. These domains are actually smaller regions of magnetization that are either parallel or antiparallel to the overall magnetization of the material. Depending on this direction, the bubble indicates either a one or a zero, thus serving as the units of the binary number system used in computers.

Magnetic materials are also important constituents of video tapes and disks on which data are stored. In addition to the atomic-sized magnetic units used in computers, large, powerful magnets are crucial to a variety of modern technologies. Powerful magnetic fields are used in nuclear magnetic resonance imaging, an important diagnostic tool used by doctors. Superconducting magnets are used in today's most powerful particle accelerators to keep the accelerated particles focused and moving in a curved path. Scientists are developing magnetic levitation trains that use strong magnets to enable trains to float above the tracks, reducing friction. Magnetoresistive materials has recently become popular for magnetic recording and reading heads in technologic devices.

2.4 Magnetoresistance

In 1879 Edwin H. Hall discovered that when he placed a conducting strip carrying a current in a magnetic field, a potential difference was produced across the strip - transverse to the current and magnetic field directions.

Magnetoresistance is the relative change in electrical resistance of a material on the application of magnetic field. The physical origin of the magnetoresistance is spin-orbit coupling. The magnetoresistance ratio is defined as

$$\mathrm{MR}=\frac{\Delta R}{R}=\left[\frac{R_H - R_0}{R_0}\right] \mathrm{x}100\ \% \qquad (2.5)$$

R_H and R_0 are the resistances measured in a magnetic field H and zero fields.

Magnetoresistance measurements are done with the measuring current i, and applied field H. If the field H is applied parallel to the current in sample, a longitudinal magnetoresistance is measured. If the field H is applied perpendicular to the current in sample, a transverse magnetoresistance is measured. All nonmagnetic metals exhibit an increase in electric resistance as a function of applied field. The

magnetoresistance of conventional materials is quite small proportional. Transverse magnetoresistance is larger than the longitudinal one.

The ordinary magnetoresistance effect depends only on the direction and magnitude of the applied field whereas in ferromagnetic materials anisotropic magnetoresistance effect depends on the direction of the magnetisation vector. While the longitudinal magnetoresistance effect is a result of the increase in the resistance of material, the transverse effect is a result of the decrease in the resistance of material. The anisotropic magnetoresistivity is generally described as the difference between the longitudinal and transverse magnetoresistances.

Normal magnetoresistance, the more common version, involves a change in resistance on the order of 1%. Recently, new types of magnetoresistance have been discovered. In the late 1980s two European scientists working independently, Peter Gruenberg of the KFA research institute in Julich, Germany, and Albert Fert of the University of Paris, discovered what was to be called giant magnetoresistance (GMR [20, 21]. They saw resistance changes of 6 to 50% in materials comprised of alternating very thin layers of various metallic elements. Recently scientists have discovered magnetoresistive effects on the order of 1000% - so-called colossal magnetoresistance (CMR) [22]. Magnetoresistance has aroused great interest recently because of possible application in devices such as read/write heads in computer discs and in sensors.

2.4.1 Giant magnetoresistance

Like other magnetoresistive effects, giant magnetoresistance (GMR) is the change in electrical resistance of some materials in response to an applied magnetic field. It was discovered that the application of a magnetic field to magnetic metallic multilayers such as Fe/Cr and Co/Cu, in which ferromagnetic layers are separated by nonmagnetic spacer layers of a few nm thick, results in a significant reduction of the electrical resistance of the multilayer. This effect was found to be much larger than other magnetoresistive effects that had ever been observed in metals and was, therefore, called “giant magnetoresistance”. In Fe/Cr and Co/Cu multilayers the magnitude of GMR can be higher than 100% at low temperatures.

The change in the resistance of the multilayer arises when the applied field aligns the magnetic moments of the successive ferromagnetic layers, as is illustrated schematically in the figure (Figure2.3 below). In the absence of the magnetic field

the magnetizations of the ferromagnetic layers are antiparallel. Applying the magnetic field, that aligns the magnetic moments and saturates the magnetization of the multilayer, leads to a drop in the electrical resistance of the multilayer.

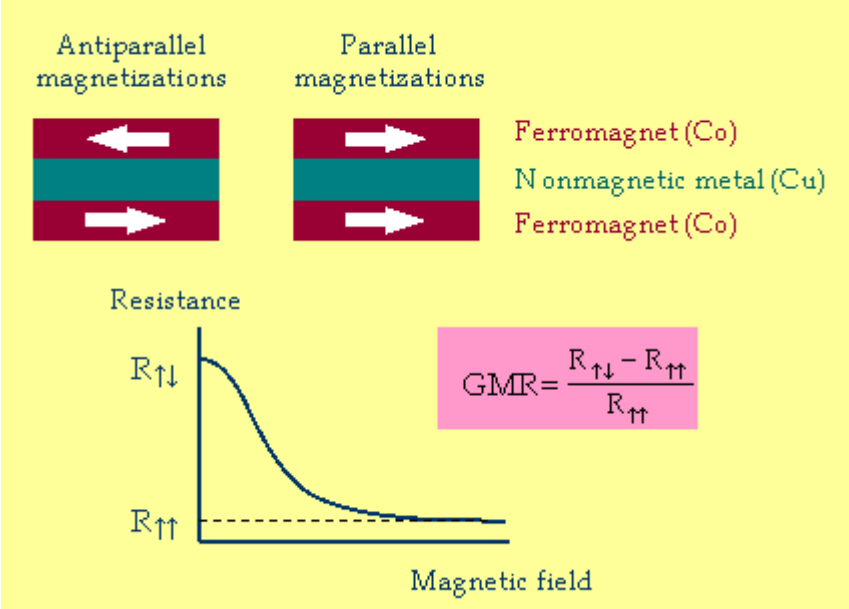

Figure 2.3 Change in the resistance of ferromagnetic layers (GMR)

GMR was also observed in equated granular nanocrystalline materials (Berkowitz et al. 1992). In multilayer systems the antiferromagnetic alignment of the ferromagnetic layers in zero fields becomes ferromagnetic as the field is applied and causes a decrease in resistance.

Granular magnetic materials composed of magnetic nanoparticles embedded in a nonmagnetic matrix show interesting physical properties, such as superparamagnetism (SPM), giant magnetoresistance and giant magneto impedance. An external field rotates the magnetic axes of all magnetic particles. The rotation towards complete alignment of all magnetic axes again reduces the resistance in a similar way as for multilayers.

Granular magnetic solids therefore show isotropic giant magnetoresistance (GMR) in non-multilayer magnetic systems. It is shown in Figure 2.4 a representation of GMR which occurs in magnetically inhomogeneous media containing nonaligned ferromagnetic entities on a microscopic scale.

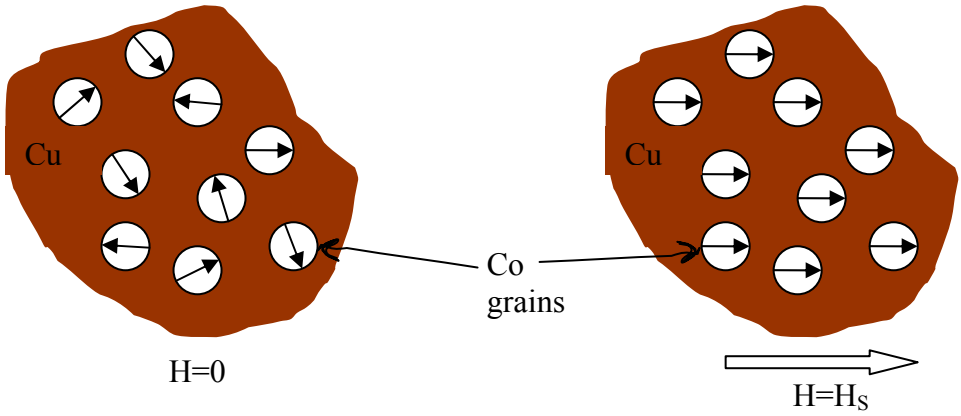

Figure 2.4 Effect of an applied field on the granular magnetic solids

The GMR in granular systems is isotropic. The explanation for the GMR is spin-dependent scattering of the conduction electrons at the ferromagnetic/nonmagnetic interfaces and, to a lesser extent, within the magnetic grains. The GMR is determined by the orientations of the magnetization axes, the density, and the size of the ferromagnetic entities. The GMR scales inversely with the average particle diameter [39]. In non-interacting grains, predominantely superparamagnetic, there should be a quadratic dependence of the relative resistance changes (ΔR/R) on the magnetization (M) of samples

$$\frac{\Delta\rho}{\rho} = \left(\frac{\rho(H,T) - \rho(0,T)}{\rho}\right) = -AF\left[\left(\frac{M}{M_s}\right)^2\right] \qquad (2.6)$$

where ρ (H, T) and ρ (0, T) are the resistivites of sample with and without the applied field H at temperature T, respectively. M_s is the saturation magnetization; A is a constant [23]. A deviation from this model is reported [24] [25]. There are a number of explanations for this deviation from quadratic behavior which include grain size distribution [26] [27] disordered surface spins under high magnetic field [28] the interaction effect between the magnetic grains [29] [30] and presence of the different magnetic phases. If a magnetic film is composed of two different phases, superparamagnetic and ferromagnetic, then the magnetization will be a function of these two phases

$$M_T(H) = (2M^S_F)\tan\left[\left(\frac{H \pm H_c}{H_c}\right)\tan\left(\frac{\pi S}{2}\right)\right] + N_g\mu\left[\coth\left(\frac{\mu H}{k_B T}\right) - \left(\frac{\mu H}{k_B T}\right)^{-1}\right] \qquad (2.7)$$

The first term describes the ferromagnetic hysteresis curve and the second term describes superparamagnetic behavior. M^S_{FM} and $M_{SPM}=N_g\mu$ is the saturation magnetization of the ferromagnetic and superparamagnetic components; S is the squareness of the ferromagnetic loop, i.e. the ratio of the remanent magnetisaition, M to M^S_{FM}. M is the average moment per grain and N_g is the number of Co grains/cm^3 in the superparamagnetic component. The magnetoresistivity expression from the equation above is obtained as

$$MR=A_{FM}\left[\left(\frac{M_{FM}(H)}{M^S_{FM}}\right)^2-\left(\frac{M^r_{FM}}{M^S_{FM}}\right)^2\right]+B_{SP}\left(\frac{M_{SP}(H)}{M^S_{SP}}\right)^2 \qquad (2.8)$$

A_{FM} and B_{SP} are the magnetorsistivity changes of ferromagnetic and superparamagnetic components respectively in infinite field. M^r_{FM} is the remanent magnetization [31]. There is worldwide research on the GMR effect. Rewievers have been published by several researchers [32] Magnetoresistive materials have important technological applications in magnetic recording and in sensors [33, 34]. Such materials have been produced as films by sputtering, as ribbons by melt-spinning, and in powder form by sol-gel methods [35, 36] and mechanical alloying M [37]. Magnetization and Mössbauer Spectroscopy measurements have been used to study magnetic and magnetoresistive properties of the granular alloys FeCu and FeAg in thin film forms. The average sizes of magnetic particles can be estimated by the coercive field.

2.4.2 Theory of GMR

GMR can be qualitatively understood using the Mott model, which was introduced as early as 1936 to explain the sudden increase in resistivity of ferromagnetic materials as they are heated above the Cruie temperature. There are two main points proposed by Mott:

First, the electrical conductivity in metals can be described in terms of two largely independent conducting channels, corresponding to the up-spin and down-spin electrons. The up-spin and down-spin electrons do not mix over long distances

and, therefore, the electrical conduction occurs in parallel for the two spin channels.

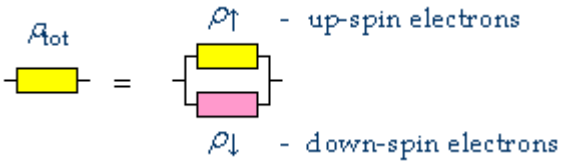

Figure 2.5 Electrical conduction occurring in parallel for the two spin channels

Second, in ferromagnetic metals the scattering rates of the up-spin and down-spin electrons are quite different, whatever the nature of the scattering centers is. The band structure in a ferromagnet is exchange split, so that the density of states is not the same for up-spin and down-spin electrons at the Fermi energy. Scattering rates are proportional to the density of states, so the scattering rates and therefore resistivities are different for electrons of different spin.

$$\rho\uparrow \neq \rho\downarrow \qquad (2.9)$$

Using Mott's arguments it is straightforward to explain GMR. We assume that the scattering is strong for electrons with spin antiparallel to the magnetization direction, and is weak for electrons with spin parallel to the magnetization direction. This is supposed to reflect the asymmetry in the density of states at the Fermi level, in accordance with Mott's second argument.

For the parallel-aligned magnetic layers, the up-spin electrons pass through the structure almost without scattering, because their spin is parallel to the magnetization of the layers. On the contrary, the down-spin electrons are scattered strongly within both ferromagnetic layers, because their spin is anti parallel to the magnetization of the layers. Since conduction occurs in parallel for the two spin channels, the total resistivity of the multilayer is determined mainly by the highly-conductive up-spin electrons and appears to be low. For the anti parallel-aligned multilayer, both the up-spin and down-spin electrons are scattered strongly within one of the ferromagnetic layers, because within the one of the layers the spin is anti parallel to the magnetization direction. Therefore, in this case the total resistivity of the multilayer is high.

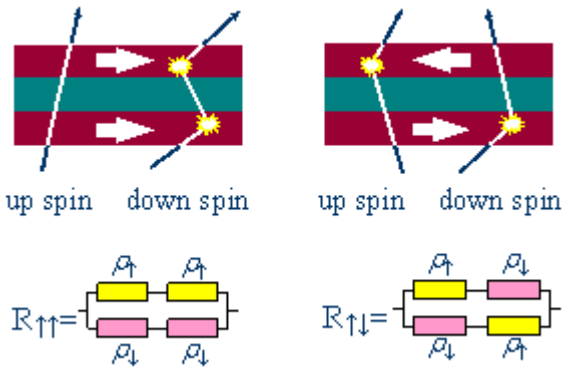

Figure 2.6 A similar picture can be visualized for the spin dependent scattering in granular magnetic alloys.

When the magnetic moments of grains are randomly oriented a high degree of scattering of anti parallel spins relative to the spins of magnetic grain is observed whereas the amount of scattering is reduced when the magnetic moments of grains are directed parallel with the application of an external magnetic field.

As a result, we can say that the origin of the giant magnetoresistance is the spin-dependent scattering at the interfaces. The importance of the interfacial scattering over the bulk scattering is believed to be due to the interfacial states and the quantum well states.

2.4.3 GMR Structures

Magnetic multilayers are composed of an alternating sequence of nonmagnetic and magnetic thin layers of only some nanometer thickness. In the last decade, these multilayer systems have got importance in magnetic sensor technology and magneto electronics due to their giant magnetic resistance (GMR) properties. Usually magnetic thin films, granular alloys and multilayer systems are prepared by means of physical deposition techniques. The method of electrodeposition offers a very cost efficient and fast way to grow ultra thin films on large area substrates.

Despite these advantages, it is not widely used in the preparation of functional thin films and film systems. One reason is that the electrochemical-grown multilayers achieve not the high GMR effects of systems prepared by physical methods, which is mainly attributed to differences in the microstructure. It could be shown for Cu/Co multilayers, that the texture of the thin grown layers is strongly dependent on the substrate and deposition conditions. Isothermal heat treatment

improves the GMR properties due to diffusion processes, which upgrade the interface between the layers and relaxation processes. Deposition under superimposing a magnetic field changes the deposition rate and structure of the layers mainly due to magneto hydrodynamic processes and yield to an increase of the magnetoelectric properties.

2.4.4 History of electrodeposition

The early history of electroplating may be traced back to around 1800. With the burgeoning knowledge and understanding of the subject of electrochemistry and its importance in understanding the processes of "electrodeposition" came the ability to deposit other metals. By the 1850's electroplating methods of bright nickel, brass, tin, and zinc were commercialized and were applied for engineering and specific commercial purposes. Thus it is said that the years from 1870 to 1940 were a quiet period as far as electroplating was concerned, significant only in gradual improvement in larger scale manufacturing processes, anodic and cathodic reaction principles and plating bath formulae. During the later years of the forties, rediscovery of heavy gold plating for electronic components took place. In comparison to that, during the mid to later fifties the usage of new and more "user friendly" plating baths based on acid formula (rather than strongly poisonous cyanide based ones) were developed and introduced for large scale commercial use [38]

Today, with the impressive progress and deeper understanding of the underlying electrochemical principles of electrodeposition, sophisticated plating baths formulas have been developed and are being routinely employed. Those provide much greater control over the working characteristics of the deposition process than hitherto. Layer thickness, performance of electroplated finishes is among the attributes that have been brought under strict control. New developments enable greater plating speed, better throwing power (the ability of a plating solution to produce a relatively uniform distribution of metal upon a cathode of irregular shape), as well as reliable plated finishes. In addition, electroplating of materials such as copper, nickel, cobalt, iron, platinum, osmium, and ruthenium are now broadly used in electronics for connectors, circuit boards, contacts etc. In general, the growth of the electronics industry as a whole, and the demand to support the expansion of its underlying infrastructure will continue to drive improvements worldwide in the

electrodeposition/electroplating industry. There has been a recent upsurge of interest in electrodeposition. This is due to four main factors/technologies:

Metal deposition for the fabrication of integrated circuits
Deposition of magnetic recording devices (heads, discs)
Deposition of multilayer structures
Deposition of nanoscale wires and similar devices

By way of illustration it is mentioned that electrodepositions of copper for integrated circuit fabrication and CuCo, CuNiCo, NiFeCu alloys or multilayers or nanowires have been successfully produced since 1997. Electrodeposition methods represent a very attractive alternative to the hitherto conventional fabrication methods.

Electrodeposition or electrochemical deposition (of metals or alloys) involves the reduction of metal ions from aqueous, organic, or fused salt electrolytes. In it's simplest form the reaction in aqueous medium at the cathode follows the equation

$$Cu^{+2}+2e^{-}==>Cu \text{ or } Co^{+2}+2e^{-}==>Co \qquad (2.10)$$

with a corresponding anodic reaction. The anode material can either be the metal to be deposited (in this case the electrode reaction is electro dissolution that continuously supplies the metal ions) or the anode can be an inert material and the anodic reaction is oxygen evolution (in this case the plating solution is eventually depleted of metal ions). The deposition may, in principle, be accomplished via two different paths: An electrodeposition process in which electrons are provided by an external power supply. An electroless (autocatalytic) deposition process in which a reducing agent in solution is the electron source. The deposition reaction presented in Equation (2.10) is a reaction of charged particles at the interface between a solid (metal) electrode and a liquid solution. The two types of charged particles that can cross the interface are metal ions "M^{+n}" and electrons "e^{-}". The deposition reaction involves four types of issues. They are: Metal-solution interface as the locus of the deposition process. Kinetics and mechanism of the deposition process. Nucleation and growth process of the metal lattice (M lattice). Structure and properties of the deposits.

The reduction of a metal, which occurs during the plating process, has been generalized as Equation (2.10) for a single metallic ion. Obviously, to reduce one mole of a given metal "n" moles of electrons are required. That is, the total cathodic charge used in the deposition "Q" (coulomb) is the product of the number of gram moles of the metal deposited "m", the number of electrons taking part in the reduction "n", Avogadro's number "N_a" (the number of atoms in a mole), and the electrical charge per electron "Q_e" (coulomb). Thus, the following equation gives the charge required to reduce "m" mole of metal:

$$Q=mnN_aQ_e \tag{2.11}$$

Now, the product of the last two terms in this equation is the "Faraday constant" "F". Therefore, the number of moles of metal reduced by charge "Q" can be obtained as:

$$m=\frac{Q}{(nF)} \tag{2.12}$$

On the other hand, the total charge used in the deposition can be obtained as the product of the current "I" (ampere) and the time of deposition "t" (second) if the deposition current is held constant. Or, if the current varies during the deposition:

$$Q=\int Idt \tag{2.13}$$

So, the number of moles deposited can be calculated as:

$$m=\frac{Idt}{nF} \tag{2.14}$$

The weight of the deposit "w" (gram) can now be obtained by multiplying Equation (2.14) with the atomic weight "M_w" of the deposited metal. Finally, to calculate the thickness of the deposit, we have to use the density of the metal "D" (gram/cm^3):

$$D=\frac{w}{V}=\frac{w}{(AT)} \tag{2.15}$$

where "V" is the volume of the deposited metal in cm^3, "A" is the area of the deposit in cm^2, and "T" is its thickness in cm. As mentioned above, if the current was held constant during the deposition, the integral in Equation (2.13), can be replaced by the simple product of current and time "I×t".

2.4.5 Electrodeposition of functional thin films and thin film systems

Electroplating has, over recent decades, evolved from an art to an exact science. This development is seen as responsible for the ever-increasing number and widening types of applications of this branch of practical science and engineering. Some of the technological areas in which means and methods of electroplating constitute an essential component are all aspects of electronics: macro and micro, optics, opto-electronics, and sensors of most types, to name only a few. In addition a number of key industries such as the automobile industry (that uses for example chrome plating to enhance the corrosion resistance of metal parts) adopt the methods even where other methods, such as evaporation, sputtering, chemical vapor deposition (CVD) and the like are an option. That is so for reasons of economy and convenience. By way of illustration it should be noted that that modern electroplating equips the practitioner with the ability to predesign the properties of surfaces and in the case of electroforming those of the whole part. Furthermore, the ability to deposit very thin multilayers (less than a millionth of a cm) via electroplating represents yet a new avenue of producing new materials.

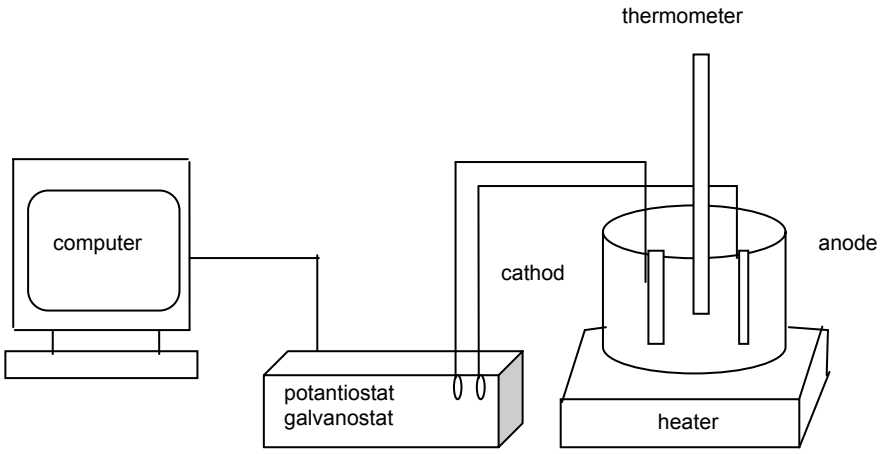

Figure 2.7 Schematic diagram of electrodeposition system

Electroplating is often also called "electrodeposition", and the two terms are used interchangeably. As a matter of fact, "electroplating" can be considered to occur by the process of electrodeposition. Electrodeposition is the process of producing a coating, usually metallic, on a surface by the action of electric current. The deposition of a metallic coating onto an object is achieved by putting a negative

charge on the object to be coated and immersing it into a solution which contains a salt of the metal to be deposited (in other words, the object to be plated is made the cathode of an electrolytic cell). The metallic Figure 2.7. Schematic diagram of electrodeposition technique.

To further illustrate the foregoing, let us assume that one has an object made of one of the common metals, like copper, and that it has been properly pre-cleaned. We should want to plate it with, say, nickel. A wire will have to be attached to the object while the other end of the wire should be attached to the negative pole of a battery (or a power supply). To the positive pole of the battery (or power supply) we connect another wire with its other end connected to a rod made of nickel. Next we fill the cell with a solution of the metal salt to be plated. It is possible to use a molten salt and in some not so common cases, such as the deposition of tungsten, that is what is done. In most, more common, cases though the salt is simply dissolved in water. In our present example the nickel chloride salt dissociates in water to positively charged nickel cations and negatively charged chloride anions. As the object to be plated is negatively charged it attracts the positively charged nickel cations, and electrons flow from the object to the cations to neutralize them (to reduce them) to metallic form. Meanwhile the negatively charged chloride anions are attracted to the positively charged nickel rod (known as the anode of the electrolyte cell). At the anode electrons are removed from the nickel metal, oxidizing it to the nickel cations. Thus we see that the nickel dissolves as ions into the solution. That is how replacement nickel is supplied to the solution for that which has been plated out and one retains a solution of nickel chloride in the cell. Nickel chloride is used here to exemplify the process of electroplating for a number of reasons. First among those is simplicity. It is not recommended; however, that nickel is used for, say, school science demonstrations because some individuals are quite allergic to it. We further do not recommend that chloride salts be used because those are amenable to release chlorine gas. For school or amateur type demonstration we recommend plating copper coins with zinc or nickel coins with copper.

2.4.6 Electrolytic Methods

Where the free energy contained within the system generates the analytical signal, electrolytic methods are an area of electro analytical chemistry in which an external source of energy is supplied to drive an electrochemical reaction which would not normally occur. The externally applied driving force is either an applied potential or current. When potential is applied, the resultant current is the analytical signal; and when current is applied, the resultant potential is the analytical signal. Techniques which utilize applied potential are typically referred to as voltammetric methods while those with applied current are referred to as galvanostatic methods.

2.4.7 Potentiometry:

Potentiometry is the field of electro analytical chemistry in which potential is measured under the conditions of no current flow. The measured potential may then be used to determine the analytical quantity of interest, generally the concentration of some component of the analyzed solution. The potential that develops in the electrochemical cell is the result of the free energy change that would occur if the chemical phenomena were to proceed until the equilibrium condition has been satisfied.

$$\Delta G_{rxn} = -nFE_{rxn} \tag{2.16}$$

This concept is typically introduced in quantitative analysis courses in relation to electrochemical cells that contain an anode and a cathode. For these electrochemical cells, the potential difference between the cathode electrode potential and the anode electrode potential is the potential of the electrochemical cell.

$$E_{cell} = E_{cathode} - E_{anode} \tag{2.17}$$

If the reaction is conducted under standard state conditions, this equation allows the calculation of the standard cell potential. When the reaction conditions are not standard state, however, one must utilize the Nernst equation to determine the cell potential.

$$E_{cell} = \frac{E^0 - RT}{nF \ln(K_{eq})} \tag{2.18}$$

Physical phenomena which do not involve explicit redox reactions, but whose initial conditions have a non-zero free energy, also will generate a potential. An example of this would be ion concentration gradients across a semi-permeable membrane. This can also be a potentiometer phenomenon, and is the basis of measurements that use ion-selective electrodes.

$$E_{mem} = (\text{constant}) - \frac{RT}{z_i F \ln(a_i)} \tag{2.19}$$

The Nernst equation relates the effective concentrations (activities) of the components of a cell reaction to the standard cell potential. For a simple reduction of the form $M^{n+} + ne^{ñ} \rightarrow M$, it tells us that a half-cell potential will change by 59/n millivolts per 10-fold change in the activity of the ion. Ionic concentrations can usually be used in place of activities when the total concentration of ions in the solution does not exceed about about 0.001M. In those reactions in which H^+ or OH^- ions take part, the cell potential will also depend on the pH. Plots of E vs. pH showing the stability regions of related species are very useful means of summarizing the redox chemistry of an element.

2.4.8 Voltammetric Methods:

Voltammetry refers to the measurement of current that result from the application of potential. Unlike potentiometry measurements, which employ only two electrodes, voltammetric measurements utilize a three electrode electrochemical cell. The use of the three electrodes (working, auxillary, and reference) along with the potentiostat instrument allows accurate application of potential functions and the measurement of the resultant current. The different voltammetric techniques that are used are distinguished from each other primarily by the potential function that is applied to the working electrode to drive the reaction, and by the material used as the working electrode. Common techniques;

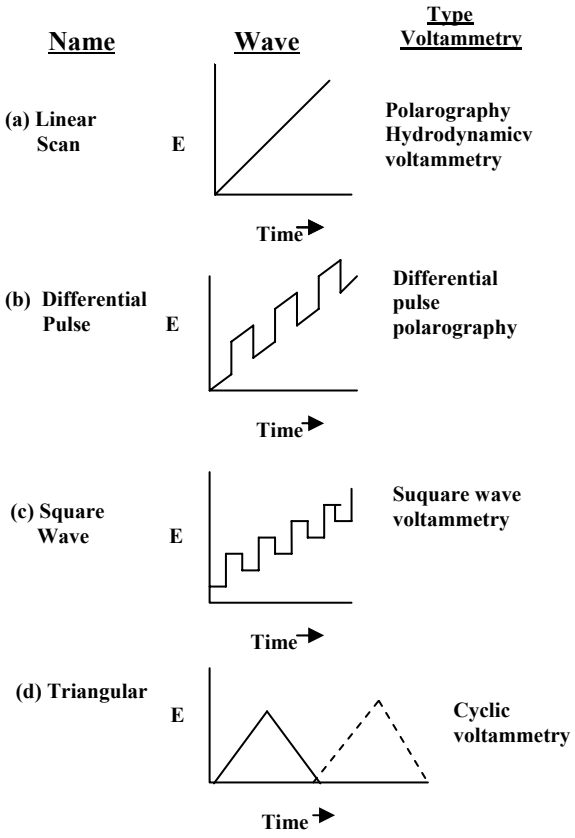

Figure 2.8 Schematics of different voltammetric techniques

Voltammetry is widely used by inorganic, physical and biological chemists for non-analytical measurements such as fundamental studies of oxidation-reduction processes in various electrolytes, adsorption processes on surfaces, and electron-transfer mechanisms at chemically modified electrode surfaces and pharmaceutical applications.

In voltammetry, the potential (excitation signal) is varied to yield a current response from the electrode; these excitation signals are applied as waveforms and the 4 most common excitation signals are: linear, differential pulse, square wave and triangular (cyclic).

CHAPTER 3

EXPERIMENTAL PROCEDURE

3.1 Sample Preparation

CuAgCo granular alloy films were prepared by electrodeposition technique. A home made computer controlled potansiostat/galvanostat was used in the preparation of the films. The films were electrodeposited on to an aluminum substrate (working electrode). Before electrodeposition the substrate was subjected to a cleaning procedure as follows:

-Aluminum foil was mechanically polished to remove any oxide layer with a zero-grade emery paper.

- It was washed with the pure water and then degreased 5 minutes in methanol

- It was dipped 30 second into 10%NaOH

- It was cleaned with pure water

-1 cm^2 area of Al foil was selected and the remaining part and back side of substrate was covered with the nail polish

- After cleaning process, substrate immediately transferred into the bath.

Three sets of CuAgCo films were electrodeposited from a citrate bath: i) In the first set, the Co content in the bath was varied from 25 to 50g/l while the other bath components of $CuSO_4$ (30g/l), Ag nitrate (0.1g/l), $MgSO_4$ (24.4g/l), H_3O_4 (6.6g/l) were kept constant. The bath pH=5.6 and the deposition current of 3.5 mA/cm^2 were applied. ii) The second set of the films was prepared with the variation of the bath pH between 5.2 and 6 while the bath Co content was taken as 25 g/l and the remaining components as in (i). iii) In the third set of the films, the deposition current was varied between 1 to 4.5mA/cm^2 and the pH value of bath was chosen as 5.6 at which

a good quality film was started to emerge. The other components of the bath were taken as in (ii).

The potansiostat/galvanostat was controlled via a visual basic program written at the Department of Engineering Physics. Deposition was performed in a constant current mode for 45 minutes in all the three sets. No agitation to the bath was applied. A 3cmx4cm platinum foil was used as anode (counter electrode). The gap between cathode (working electrode) and anode was 5cm. After deposition, the films were immediately washed with pure water and dried with a soft tissue. The super glue was applied as the support on the film surface and left to dry for 10 minutes. The film was then stripped off the substrate in a 10% NaOH solution.

From the stripped film, a 4mmx4mm part for the composition, structure and magnetorezistance characterization was carefully selected and cut by a sharp knife from the various crack free parts of the film area of $1cm^2$. The composition and structure characterization were done by a scanning electron microscopy. The magnetorezistance measurements were performed with the four terminal methods using a nanovoltmeter and a 2T home-made electromagnet. The four point contacts were made through the application of silver paste. A magnetic field of 0 to 10kOe was directed in the film plane either parallel (longitudinal geometry) or perpendicular (transverse geometry) to the constant current of 5mA in the magnetoresistance measurements. The nanovoltmeter and electromagnet were switched on 1 hour ago before any measurement. The MR measurements were repeated and checked several times by reversing the current and magnetic field directions to eliminate the heat effect and to ensure the precision of the measurements.

3.2 Sample Characterization:

For the composition and structure analyses, the scanning electron microscopy technique was employed. From the EDX (energy dispersive x-ray analysis) measurements associated with the SEM measurements, the three types of the CuAgCo films were found to be composed of mainly CuCo alloy diluted with ~1% Ag component. The SEM measurements showed that our electrodeposited CuAgCo films have the granular structure. The spherical shape of granules was detected in the films. The results of EDX, SEM and magneto transport measurements are presented in the following sections.

CHAPTER 4

RESULTS, ANALYSIS AND DISCUSSION

4.1 Compositional Measurements:

The composition of electrodeposited alloys depends on many parameters and differs usually from the components of the electrolyte. Five types of co-deposition are defined as i) “regular”, ii) “irregular”, iii) “equilibrium”, iv) “anomalous” and v) “induced” [40]. The relative proportions of metals in the bath are expected in the film in the first three types. In anomalous and induced co-deposition, the film composition differs from the expected deposition. In anomalous co-deposition the less noble metal is deposited more preferentially and its relative concentration in the alloy is higher than the bath. In induced co-deposition a particular element can be co-deposited to form an alloy and can not be co-deposited in a pure form.

The Standard electrode potentials of Cu, Ag and Co are 0.34, 0.8 and -0.28V respectively. Among these elements, the noblest material is silver and the next one is copper and then cobalt. So Ag is expected to be more preferentially electrodeposited at even very small electrode potentials.

Although there is not much work on electrodeposited CuAgCo alloys in literature; some studies on the electrodeposited AgCo, CuAg, AgCuCo films are reported. The studies on the Ag containing films report that the amount of Ag component in the films prepared with the constant current regime depends on the deposition conditions: The electrodeposition of an 80% of Ag from a sulfate bath of 0.0528 g/l $AgSO_4$ was reported in an AgCo film on Al substrate [41]; using 12g/l of $AgNO_3$ in a bath, more than 95% of Ag concentration was obtained in an alloy film of FeAg on Al substrate [42]; a 3.5% Ag concentration in a film of CuAg alloy was achieved from a bath with 0.5 g/l $AgNO_3$ [43]; a 45% Ag content from a citrate electrolyte with 0.5 g/l $AgNO_3$ was reported in a film of AgCuCo nanowires into porous aluminum oxide membrane [44].

Our CuAgCo films were deposited with the constant current mode from a citrate bath of 0.1 g/l $AgNO_3$ as it was mentioned in the previous section. Figure 4.1 shows the compositions of the films determined using Energy Dispersive X-ray analysis (EDX). The concentration of Ag was detected to be around 1 at. % in all the three types of films, indicating almost no effect of neither Co concentration, nor pH nor the deposition current on the amount of Ag concentration in the films. By increasing Ag content (more than 0.2g/l $AgNO_3$) in the bath, an increase in the amount of Ag beyond 1% in the films was aimed but the attempt resulted in very fragile and dark films causing difficulty in separating them from their substrate without the damage of cracks. The magnetic films for this study were therefore prepared by keeping Cu (30g/l) and Ag (0.1g/l) components constant and varying the bath Co content or pH or deposition current.

As it can also be seen from the figure, the Co concentration increases with increasing Co content in the bath and with the deposition current while the Cu concentration decreases with these variables. When the concentrations of Co and Cu in the film are compared with that of in the electrolyte, it can be seen a direct proportional relation between the concentrations of these metals in these depositions. The deposition behaviors of Co and Cu therefore resemble to the regular co-deposition of alloy as described in [40]. The Co concentration in the films prepared with the variation of pH increases first, it then becomes constant reaching a saturation value of 20 at. % above pH=5.5 which is less than the Co concentration in the electrolyte indicating again the regular deposition.

It is also obvious in Figure 4.1 that most of the films prepared with the variations of the bath Co content and the deposition currents above 3mA/cm^2 have higher Co concentration than the films of pH variation.

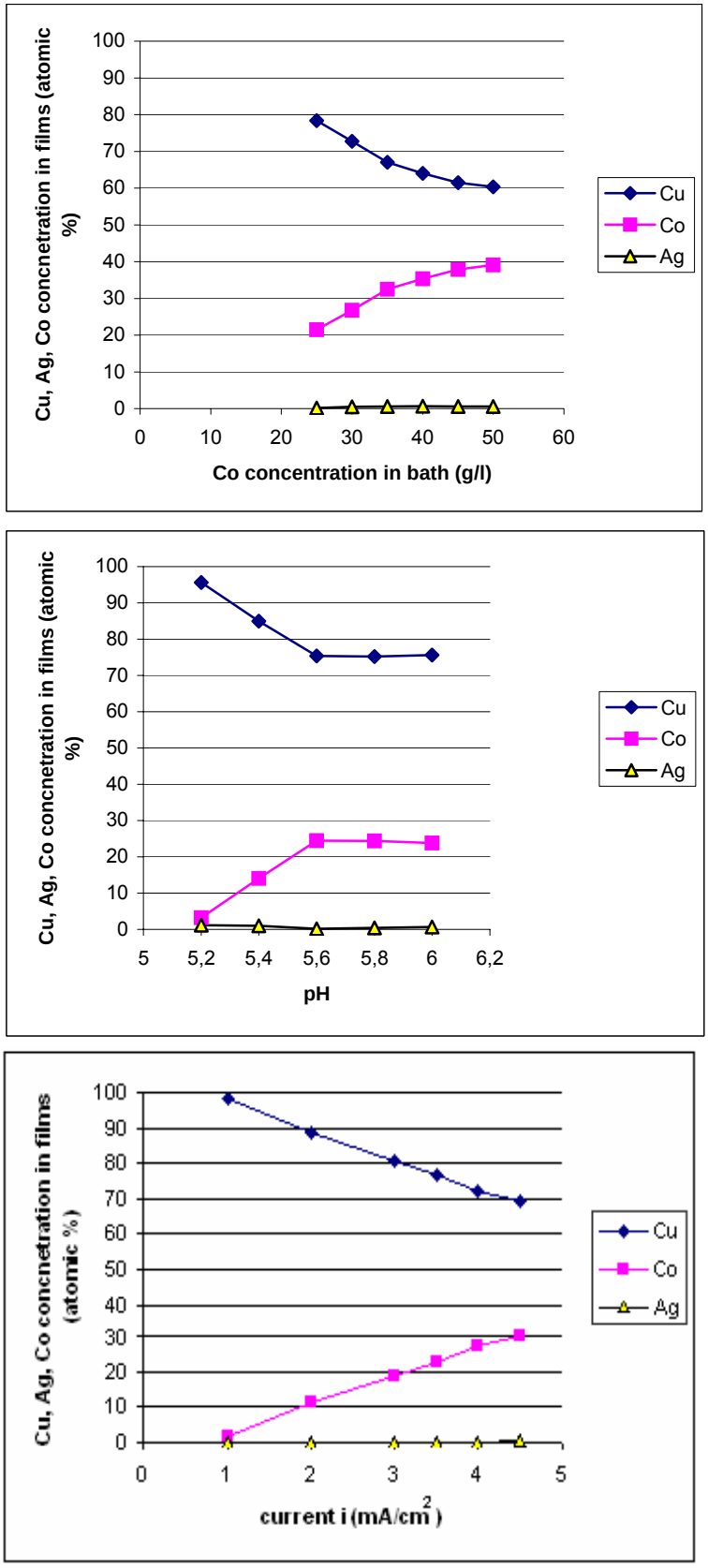

Figure 4.1 The variaiton of Cu, Ag and Co concentration in films as functions of Co content in bath, pH and deposition current

The small Ag concentration in our films detected to be ~1% is a similar result to [43] but controversial to [41, 42, 44]. It is especially interesting that although we deposit our CuAgCo alloy films with a similar electrolyte to that in [44], we obtained a different composition profile (with 1% Ag) on a different type of substrate than the films (with 45% Ag) in [44]. One possible explanation to this might be as follows: Since silver (M=107.868 g/mol) has higher atomic weight than copper (63.546 g/mol) and cobalt (58.9332g/mol), it might be reasonable to think that in the absence of agitation, the transfer and therefore deposition of the nobler Ag atoms (0.1g/l in the bath) were limited by the much more mass transfer of the lighter and dominant Cu (30 g/l in the bath) and Co (25-50 g/l in the bath) components in the bath.

4.2 SEM Measurements:

Figure 4.2 shows some examples of SEM (scanning electron microscopy) photographs of the three types of electrodeposited CuAgCo film. The granular structure is clearly seen in these photographs. The spherical example of the grains of CuAgCo alloy detected in our films is shown in Figure 4.2a. Spherical and elongated grain structures were also reported in CuCo films prepared at low current density of around 3mA/cm^2 and at higher current density of 8mA/cm^2 respectively [45].

In our films for the deposition current less than 2 mA/cm^2, a non-connected network of grains was observed as an example of that can be seen in Figure 4.2c. The MR effect in these films could therefore not be measured although electrical conduction was good with a resistance of higher than 30Ω.

The film formation on the substrate of these films starts first as the creation of nucleation at different sites of the substrate and as the deposition continues, the nuclei grows, form grains and the grains eventually are connected to each other. Due to increasing current density, the electrode polarization increases, this results in an increase in the throwing power and the plating solution gains the ability of filling small spaces. The current density therefore plays an important role in the formation of a dense nucleation and fine grain size. If the deposition current density is insufficient the density of nuclei is expected to be low resulting in a less grain density and large grain sizes. The non-connected network seen in some of our films may therefore be attributed to the insufficient current density < 2mA/cm^2 which is

unable to start enough nucleation. Uniformly connected grains in the CuAgCo films were however obtained for the different deposition parameters of bath Co concentration, pH and current density above 2mA/cm^2.

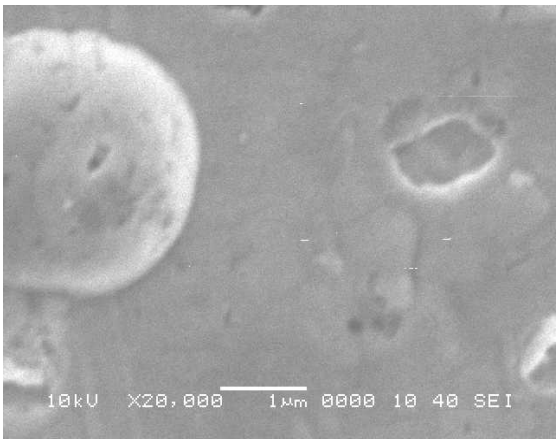

(a)

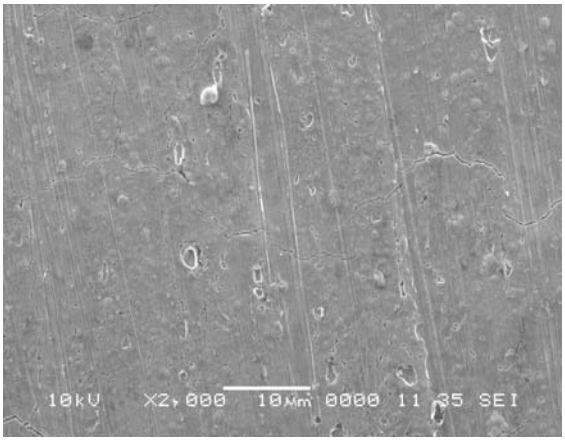

(b)

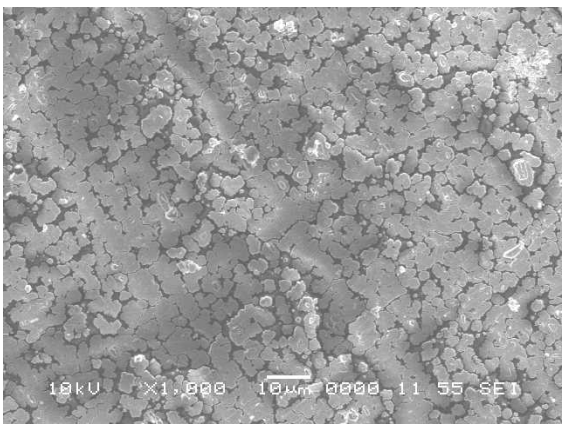

(c)

Figure 4. 2 SEM photographs of CuAgCo films. a) 35 g/l Co in bath, b) pH= 5.6, c) 1 mA/cm^2 deposition current

4.3 Magnetoresistance Measurements:

As it is explained in Chapter 2, magnetoresistance (MR) effect in a magnetic film is usually observed as two kinds: i) the first type is the effect of an applied field on the trajectory of the conduction electrons due to the Lorentz force. This type generally shows a directional dependent scattering because of the spin-orbit coupling and results in anisotropic magnetoresistance (AMR) effect, ii) the second type is a direction independent effect caused by a dominant spin dependent scattering. In this type the spins of conduction electrons are influenced by the local magnetic fields. The spin dependent scattering is therefore expected at the interface or at the grain boundaries and named as the "giant" (due to its relatively high magnitude when compared with the ordinary MR) magnetoresistance. In the first type, the MR is positive when it is measured in the longitudinal geometry but negative when measured along the transverse direction. The GMR effect has a negative and equal magnitude at the same magnetic field regardless of the measuring directions and geometries.

The MR (and therefore GMR) effect has a close relation to the magnetic coupling mechanism in a granular film. When the exchange coupling is strong enough, a ferromagnetic domain structure is created within the grains or among the grains. The film is then described as ferromagnetic one. The magnetization rotation is relatively easier in these films because of a low coercive field. The grain size plays an important role in the formation of domains. When the grain size is above a critical value, a multidomain grain is expected. A single domain grain is formed when the grain gets a critical size. The coercive field is generally high and the rotation of magnetization is therefore relatively difficult in these films. When the size of grain is reduced below the critical size, a superparamagnetic grain structure is obtained. A superparamagnetic grain may have a single magnetic domain and its magnetization vector is a time dependent quantity which may behave as it is a single paramagnetic particle as indicated in Chapter 2. When the magnetization vectors within the film are coupled antiparallely, an antiferromagnetic structure is obtained.

The spin dependent scattering mechanism which is the source of the GMR effect is therefore closely related to the magnetic structural formation within the films. An antiferromagnetic coupling gives a high spin dependent scattering and

therefore gives a high GMR effect while ferromagnetic coupling results in relatively low and easily saturating MR (see Chapter 2). The superparamagnetic structure has relatively difficult magnetization rotation in low field and gives a relatively small GMR effect but a high value of an unsaturated GMR may be obtained at high fields. The shape of GMR versus applied field curve depends on the magnetic structure in the film. A relatively low and easily saturating shape is attributed to the ferromagnetic domination while an easily saturating and a cusp-like shape is related to the dominantly antiferromagnetic formation. The GMR-H graph of a dominant paramagnetic structure shows mostly an unsaturated almost straight line or unsaturated cusp-like shape.

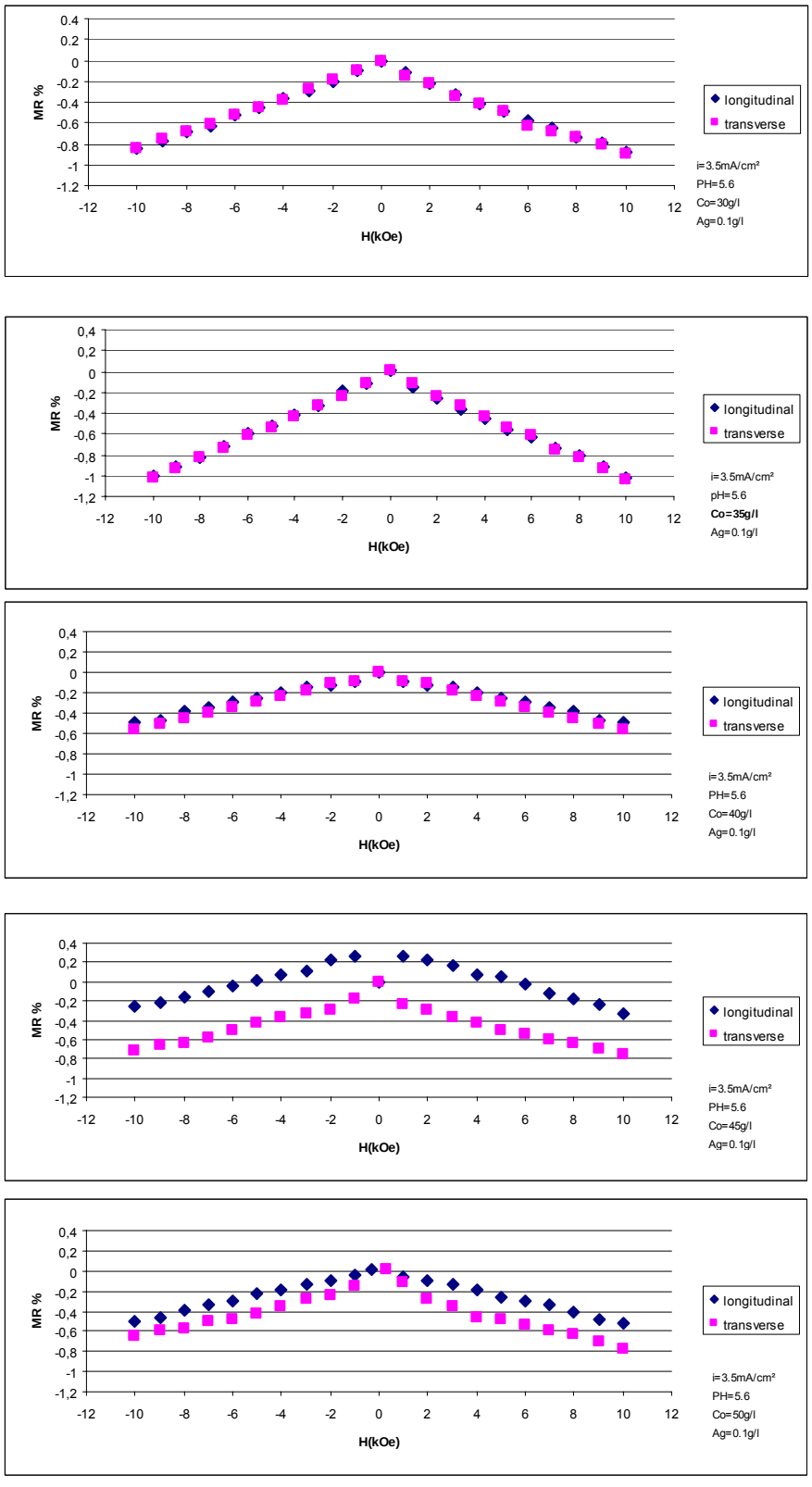

Figure 4.3 The MR graphes as a function of Co content in bath

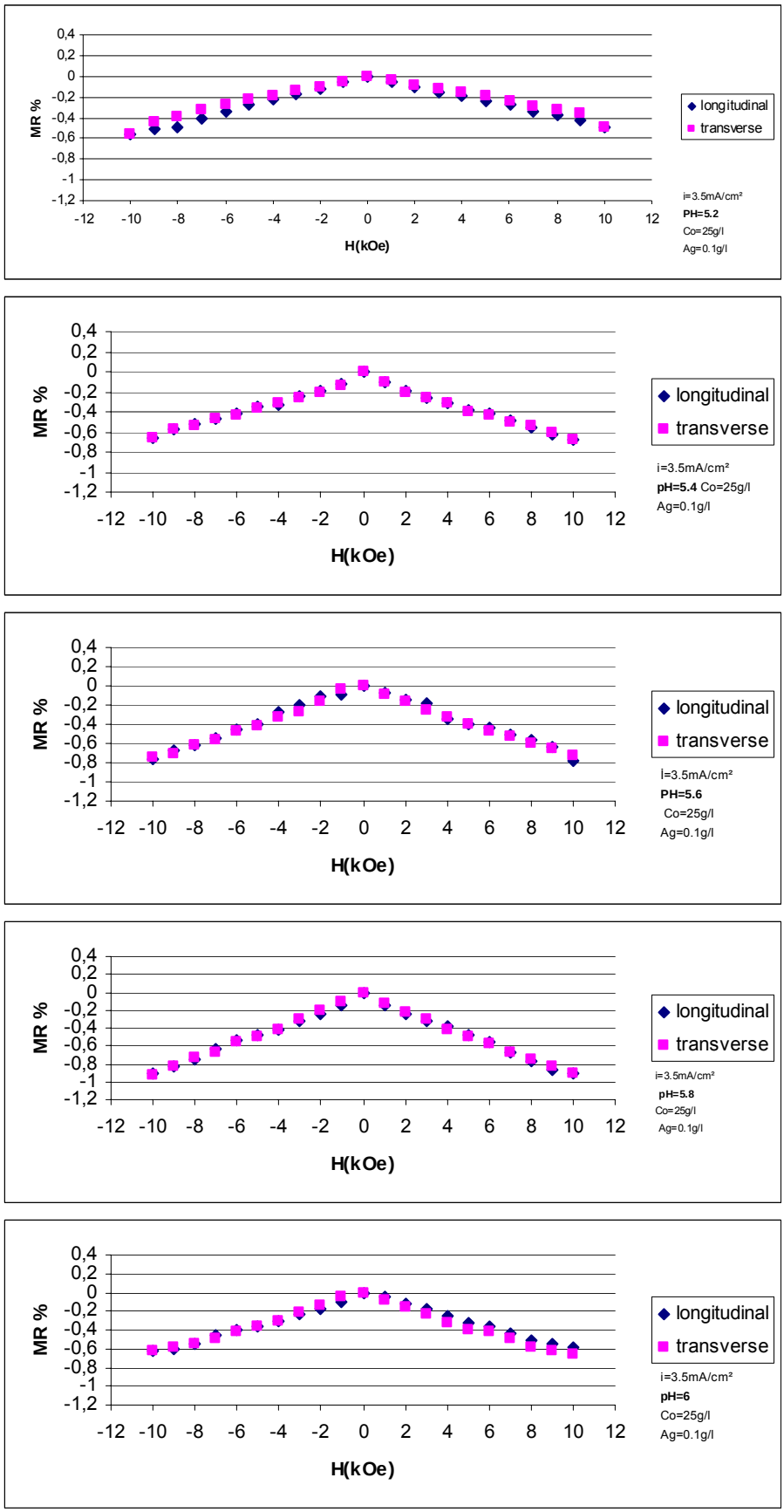

Figure 4. 4 The MR graphes as a function of pH

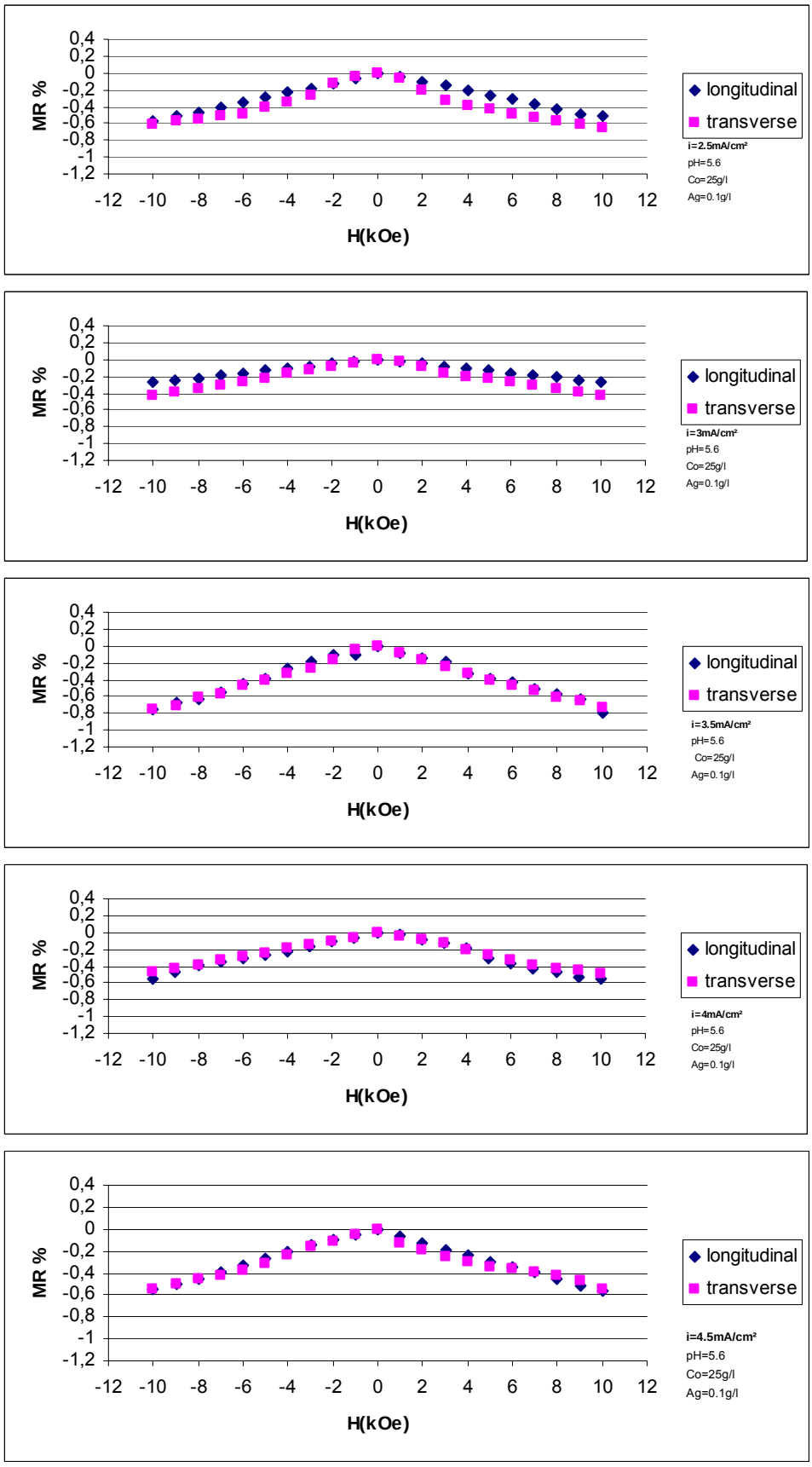

Figure 4. 5 The MR graphes as a function of the deposition current density

We measured the MR effect in our films at room temperature under the magnetic field variation up to 10kOe. The MR measurements were performed in the longitudinal and transverse geometries using a 2T home-made electromagnet. The MR variation with the applied field for the films of the different Co content in bath, pH and the deposition current density are shown in Figure 4.3, 4.4 and 4.5 respectively. A very slight cusp-like (bell-like) shape is detected in some of the transverse MR curves of the current variation graphs but the general shape of the MR curves is a linear decreasing line with increasing magnetic field. In the Co content variation, the longitudinal and transverse MR lines are almost the same. This means both measurements indicate a negative and increasing MR effect up to a Co content of 35g/l in the bath. Beyond that concentration, the MR lines of longitudinal and transverse measurements differ from each other with increasing applied field and the longitudinal measurement gets positive values at low field but returns back to negative values which indicate the presence of an AMR component as well as GMR component in these films. In the graphs of MR effect in the films of pH variation (Figure 4.4), the longitudinal and transverse lines do not differ much from each other. This means that there is no AMR contribution to the MR graph while the main contribution comes from the GMR effect in these samples. In the MR lines of the films of current variation (Figure 4.5) a slight AMR effect is also detected in the films of i = 2.5 and 3 mA/cm^2. The GMR component is the dominant component in these films again. The absence of AMR effect in the films indicates that the spin dependent scattering is the major contributor. Although we observe a dominant GMR effect and an AMR component in some of our films, no saturation in the MR effect is detected which is another indication of a superparamagnetic behavior. The GMR values at 10kOe in each type of films are given in Figures 4.6.

When the grain size is large enough caused by the connection among the magnetic particles called as “the magnetic particle coalescence”, an easily saturating MR and magnetization curves are obtained. When a distribution of magnetic particles from large enough for an easy saturation to small enough for an uneasy saturation is present, the shapes of MR and magnetization curves would most probably reflect these both features. In granular systems in which the magnetic component constitutes the diluted amount in the non-magnetic matrix, the number of large magnetic particles which are responsible for easy saturation of magnetization and MR is usually very less than (less than 10% for the as-deposited samples) that of

small magnetic particles which are responsible for the super paramagnetic behavior. The width of the peak at half height of magnetoresistance curve may also reflect the grain size distribution. The bigger the width at half maximum indicates the smaller the grain size and harder to saturate them at moderate fields. The smaller the width at half height indicates a relatively easy saturation at relatively lower fields (e.g. lower than 0.1T) The MR curves of our three type samples show no saturation and have relatively wide width at half maximum as seen in Figures 4.3, 4.4 and 4.5. These features of our unsaturated MR curves may therefore be attributed to the mostly small grain size which causes the superparamagnetic particles in these samples.

In Fig 4.6a, the MR effect at 10kOe first increases up to 35 g/l Co and then it decreases with further increase in Co concentration. This may be explained that the change in the bath composition results in a change in the film composition as can be seen from Figure 4.1 which in turn affects the MR values. The low values of MR of the films which have a low Co concentration can be ascribed to the relatively dilute Co concentrations causing to fewer magnetic non-magnetic interfacial scattering sites. The maximum MR value is obtained for the 35 g/l Co in the bath which may be regarded as corresponding to the optimum distribution of the Co granule size and inter-granule separation. Above the Co concentrations of 32 % in the films (which corresponds to 35g/l Co in the bath), we observe a decrease in the MR value as well as an AMR development is detected as can be seen in Figure 4.5. The formations of multi-ferromagnetic domains in each granule and ferromagnetically coupled Co granules are highly probable above 32% Co concentrations in CuCo films which result in an AMR effect and a decrease in the MR value [31]. The start of the formation of an AMR effect and a decrease in the MR value in our films with Co concentration higher than 32% may be attributed to the coalescence threshold of Co granules in our films.

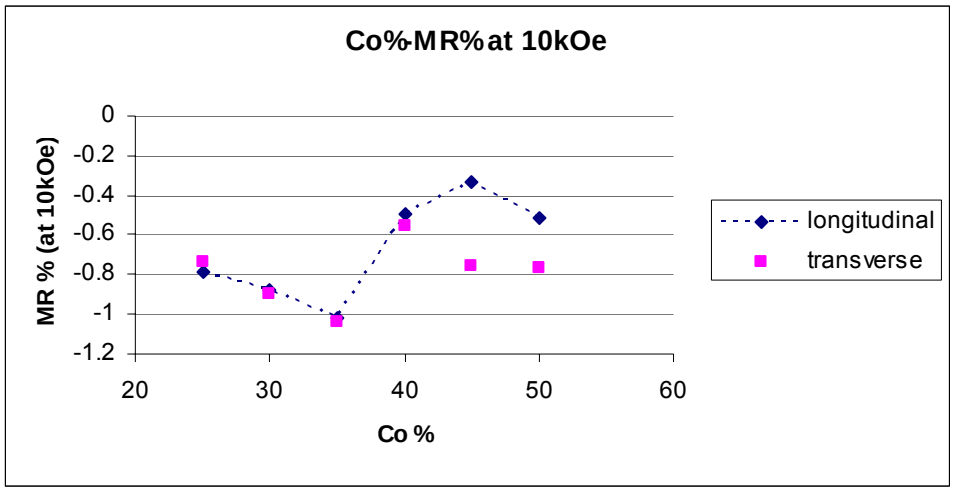

(a)

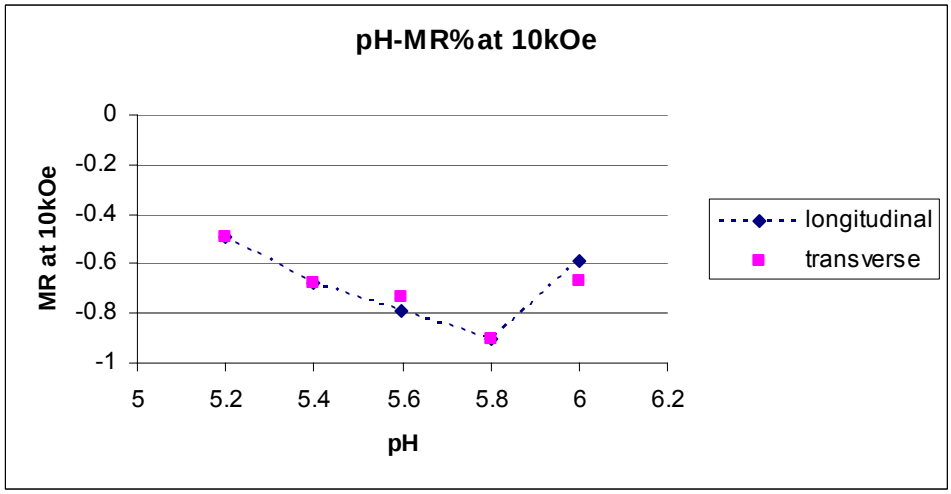

(b)

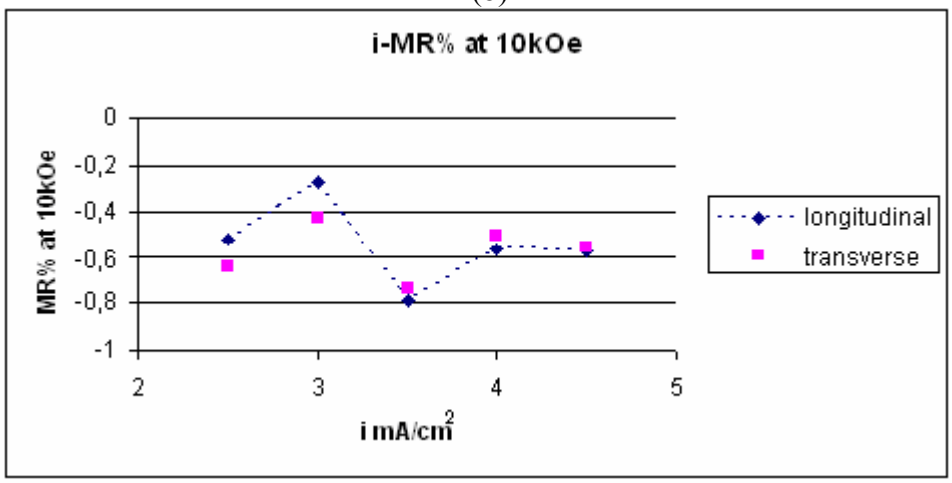

(c)

Figure 4. 6 The variation of MR at 10 kOe with the Co content in the bath, pH and the deposition current

The effect of pH on the MR value of the CuAgCo films can be seen in Figure 4.6b. The MR value increases with increasing pH up to 5.8 and then it decreases with

the further increase in pH. The Co concentration in the films also increases up to pH=5.6 and it becomes saturated beyond that pH value (Figure 4.1) but never exceeding 30% Co concentration. Again, as the Co concentration increases the number of Co atoms in each grain increases causing larger grains and reaching an optimum grain size distribution at pH=5.8 to give around 1% MR effect. Beyond this pH value, further increase in the grain size may provide a connection between the grains leading to ferromagnetically coupled regions and therefore lower MR values. We should also emphasize that a better quality film in the pH regions between 5.6 and 6 is obtained. The MR value increased in the pH=5.2 to 5.8 regions while the Co concentration in the films increased up to pH=5.6 and became constant above that value. Even if we attribute the MR increase up to pH=5.6 to the increase in the Co concentration, the further increase in MR value above pH=5.6 to 5.8 can not be ascribed to the increase in the Co concentration in the films. The different grain shape and size distributions above pH=5.6 from those below that pH value may play important role for the lower values of MR effect and a careful investigation on the grain shape and sizes should be performed to find the exact cause of the MR decrease beyond pH= 5.6.

Any regular change in the MR effect with the deposition current variation was not observed as it can be seen from Figure 4.6c. The irregular variation in MR values at 10kOe may be ascribed to the formation of the different sizes and numbers of ferromagnetically coupled grains even below 30 % Co concentrations in the films as their indications come from the detection of AMR effect and a slight cusp-like MR curve in some of the films seen in Figure 4.5.

Table-4.1 sp**,** a and c represents superparamagnetic, AMR and/or cusp-like shape present in these samples respectively.

Co variation	dMR/dH	pH	dMR/dH	i (current)	dMR/dH
25	-0.071 sp	5.2	-0.045 sp	2.5	-0.059 c a
30	-0.083 sp	5.4	-0.060 sp	3.0	-0.043 a
35	-0.102 sp	5.6	-0.071 sp	3.5	-0.071
40	-0.054 c, a	5.8	-0.088 sp	4.0	-0.054
45	-0.057 c, a	6.0	-0.065 c	4.5	-0.043 c
50	-0.072				

The slopes of the MR lines in Figure 4.3, 4.4 and 4.5 are seen to be different from each other. The slope values dMR/dH of each transverse MR lines are given in Table-4.1. The different MR slopes in our MR graphs suggest that we may have different saturation field for each sample. It is expected that the bigger dMR/dH, and therefore the bigger saturation field should give a bigger MR value at a particular field, e.g. at 10kOe, below the saturation.

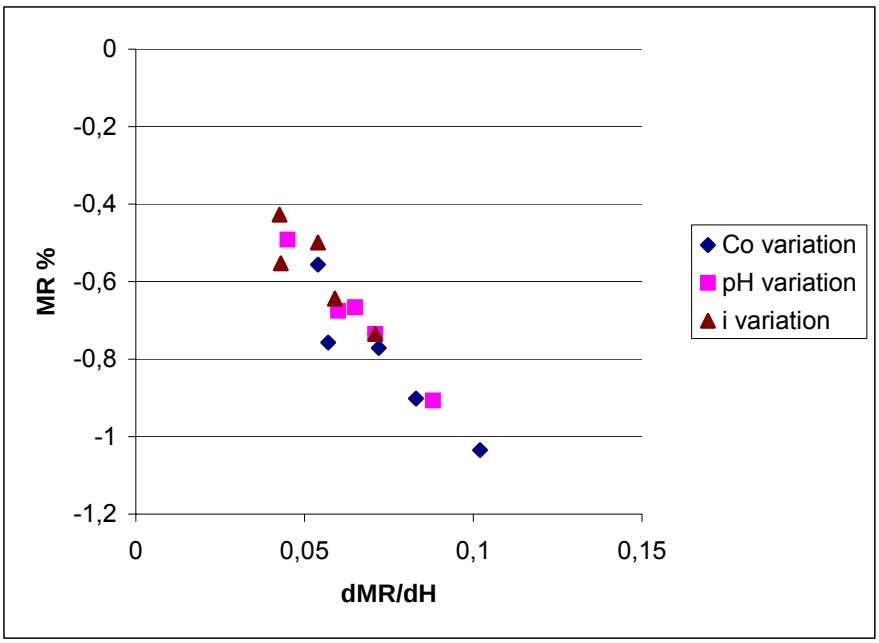

Figure 4. 7 MR variation with dMR/dH (and therefore with saturation field)

The samples which do have the Co concentrations above the coalescence threshold described above (the samples indicated with c) or AMR (indicated with a) show relatively low dMR/dH value and therefore low saturation fields.

The expected increase in the MR value at the example field of 10kOe with the increasing saturation field of the superparamagnetic films can be seen in Figure 4.7. The variation of dMR/dH with Co concentrations in the films which are assumed to be superparamagnetic in nature and do not show any presence of Co grain coalescence and AMR effect is shown in Figure 4.8 for the films of Co and pH variations.

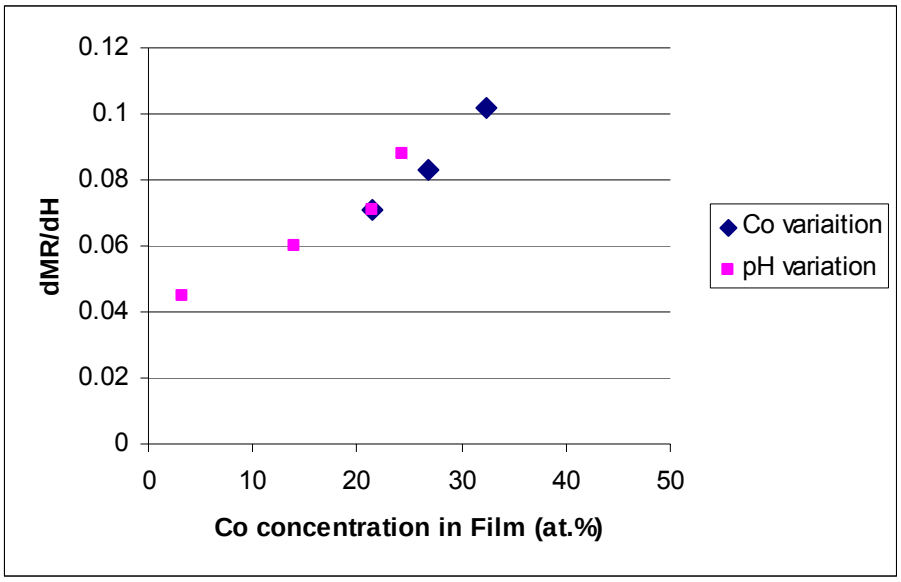

Figure 4. 8 The variation of dMR/dH with Co concentration in film.

Figure 4.8 suggests that the saturation field increases with increasing Co concentrations in the so-called superparamagnetic films. However, when the ferromagnetically coupled Co grains are generated above the coalescence threshold value of ~32% Co, a reduced value of the saturation fields is expected for the samples in which enough Co concentration leading to AMR effect is present. This seems to be reasonable because more Co presence has a higher probability of the formation of more ferromagnetic coupling which makes easier rotate the magnetization vector and therefore results in a reduced saturation field.

As it has been discussed above, in granular alloys, ferromagnetic, antiferromagnetic and superparamagnetic structures may exist together, the GMR effect may therefore result from the different sources in these samples. The GMR effect due to the antiferromagnetic structure is somewhat a larger effect when compared to the other two. An anhysteretic and isotropic MR is also related to the superparamagnetic nature [31]. In the samples which are considered to be mainly superparamagnetic, the contributions of the ferromagnetic and paramagnetic entities to the GMR are determined to be less than 10% and higher than 90% respectively [31, 46]. The coalescence threshold at which a network of ferromagnetic grains forms first is reported to be around 30-35at. % for CuCo alloys [47]. Considering the unsaturated, an hysteretic and isotropic nature of some of our samples which are

below or at the edge of threshold concentration, we decided to analyze them assuming that they have almost mainly the superparamagnetic nature.
The MR effect for superparamagnetic grains is given in Chapter 2 as

$$MR=B_{SP}L^2\left(\frac{\mu H}{kT}\right) \tag{4.1}$$

where Bsp is the saturation value of the MR which we take it as the value of MR at 10kOe in our samples. μ is the magnetic moment per superparamagnetic grain. H is the magnetic field. k is the Boltzman constant (=1,38x10^{-17} erg/ ^{o}K) and T is the temperature. L (μH/kT) is the Langevin function and given as

$$L\left(\frac{\mu H}{kT}\right)=\coth\left(\frac{\mu H}{kT}\right)-\left(\frac{\mu H}{kT}\right)^{-1} \tag{4.2}$$

The equation (4.1) is a transcendental equation and can be solved by the graphical method or by the fitting procedure. From the solution of Eq. 4.1 using our MR data, the average magnetic moment per grain, μ, is obtained for a single average component. Figure 4.9 shows the magnetic moment distribution of our superparamagnetic samples as functions of the Co concentration in bath and the bath pH.

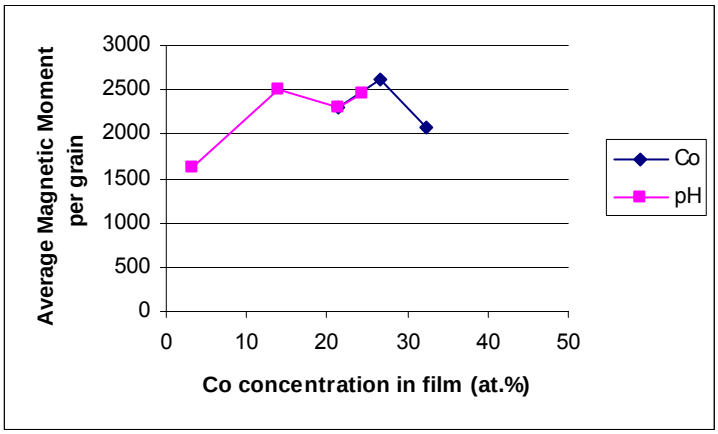

Figure 4.9 Variation of average magnetic moment as a function of Co concentration in films obtained by varying the bath Co concentration and pH.

It can be seen from Figure 4.9 that the average magnetic moment per grain increases with the bath pH. The magnitude of average magnetic moments is between

2083-2614μ_B for the Co variation while it is between 1624-2506μ_B for the pH. The magnitude of magnetic moment per grain is distributed between 1600-2500μ_B for Co concentration between 15-32 at. % in our superparamagnetic films. The Co concentrations in the film prepared with pH and deposition current variation are less than Co concentration in the films prepared with Co variation in bath (see Figure 4.1). However, in Figure 4.9, the granular average magnetic moments per Co concentration in the films prepared with the pH variation seem to be higher than that of the films prepared with the bath Co variation for the Co concentration between 20-32 at.%. This may indicate that either the density of atoms per grain or the grain size, and therefore the number of atoms per grain, of the films prepared by the pH variations is bigger than those in the films prepared with the bath Co variation.

The average volume, V_g, of superparamagnetic grains can be calculated by assuming the small Co granules of the fcc structure with the lattice constant of a_o=3.537Å, and the radii, r_g can then be obtained, assuming the granules to be spherical as suggested by the SEM analysis, using the expressions below [31].

$$V_g=N_{Co}a^{3/4} \text{ and } r_g=\left(\frac{3V_g}{4\pi}\right)^{1/3} \tag{4.3}$$

where $N_{Co}=\mu/1.72\mu_B$ is the average number of the Co atoms in a granule. Here the bulk value of 1.72μ_B is taken for the magnetic moment of the Co atom.

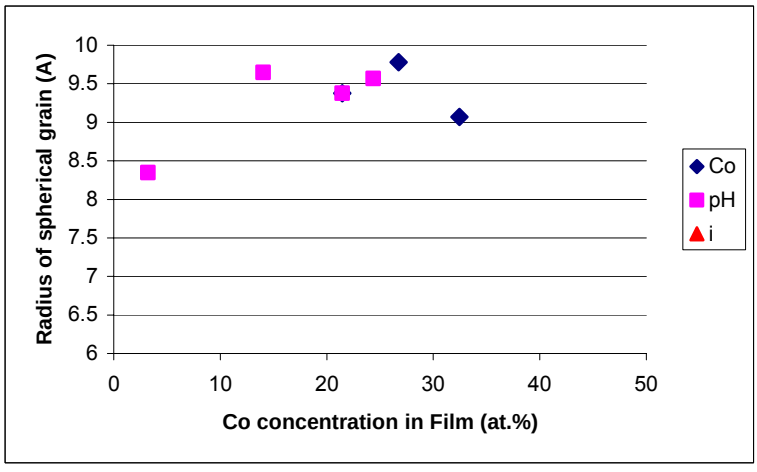

Figure 4. 10 The radius of grains as a function Co concentration in film

Figure 4.10 shows the radius of grains as a function of the Co concentration in the superparamagnetic films. The size of grains seems to be mostly placed between 9-10Å for the Co concentration between 15-32 at. %. The surface to volume ratio for a spherical granule is given as $3/r_g$ and predicted to be proportional to MR ratio [48]. The variation of the MR effect with the surface to volume ratio for a spherical grain is shown in Figure 4.11. No proportionality between the MR values and $3/r_g$ is determined.

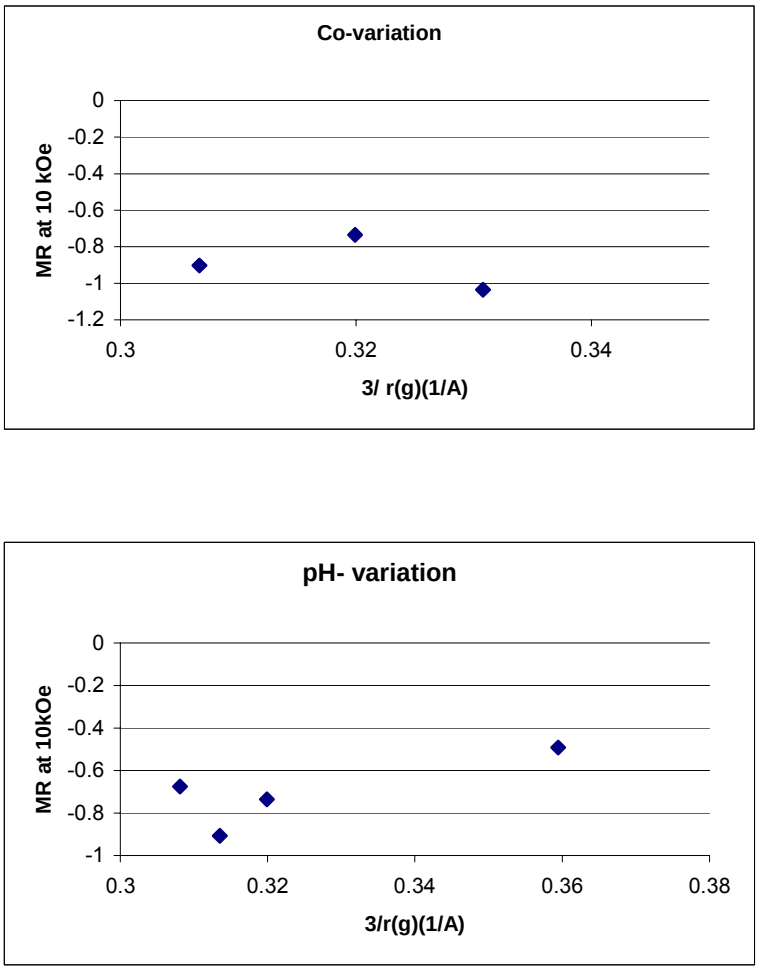

Figure 4.11 The variation of MR with surface to volume ratio $3/r_g$ for spherical grains.

The percentage grain concentration may be found from the ratio between the concentration % of atoms in the films to the average number of atoms in a grain, N_{Co}. Using the values of the percentage concentration of atoms in the films in Figure 4.1 and the $N_{Co}=\mu/1.72\mu_B$ values from Figure 4.9 we have drawn the graph of MR

against the grain concentration % for the films which do not show any AMR properties for the Co and pH variations. We do not do the same analysis for the films which show a significant AMR component. As it can be seen from Figure 4.12, a direct proportionality between the MR and the grain concentration in our films is clearly determined. This implies that the probability of the spin dependent

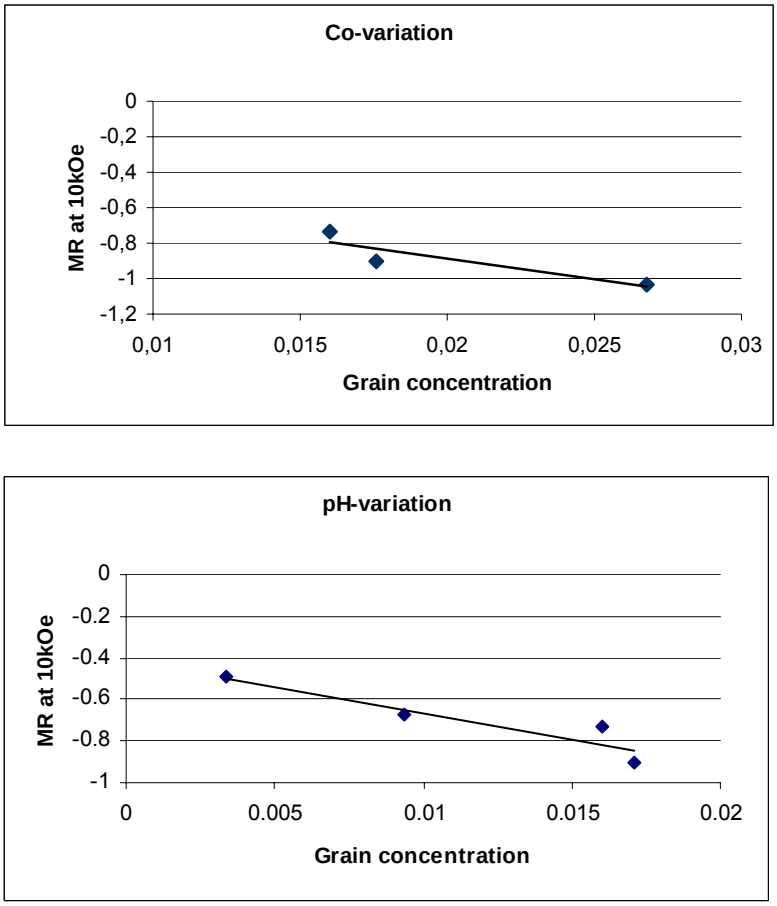

Figure4. 12 The variaiton of MR with grain average concentration

scattering becomes greater as a result of the increase in the collision probability in the interface between the conduction electrons and the superparamagnetic grains, resulting in greater values of MR under the influence of magnetic field. The increase in the MR with increasing the grain concentration is also reported in [31, 49].

4.4 Angular Variation of Magnetization:

The relation between the saturation magnetoresistance change and the initial domain arrangement is given by

$$(\frac{\Delta\rho}{\rho})_s = (\frac{3}{2})(\frac{\Delta\rho}{\rho})_{si} [<\cos^2\theta>-(\frac{1}{3})] \quad (4.4)$$

where $(\Delta\rho/\rho)_{si}$ is the greatest change observed when a sample is brought from the ideal demagnetized state to saturation [50]. Θ is the angle between the magnetization vector and the applied magnetic field. When saturation is accomplished at 10 kOe, $<\cos^2\Theta>$ gets unity. This should imply that all the magnetic moments align along the magnetic field. Assuming $(\Delta\rho/\rho)_{si}$ is the magnetoresistance value at 10kOe, and $(\Delta\rho/\rho)_s$ is the magnetoresistance value at a particular magnetic field and using our transverse magnetoresistance data which shows negative and decreasing behavior, we have calculated the angular variation $<\cos^2\Theta>$ of the magnetization vector in some of our samples.

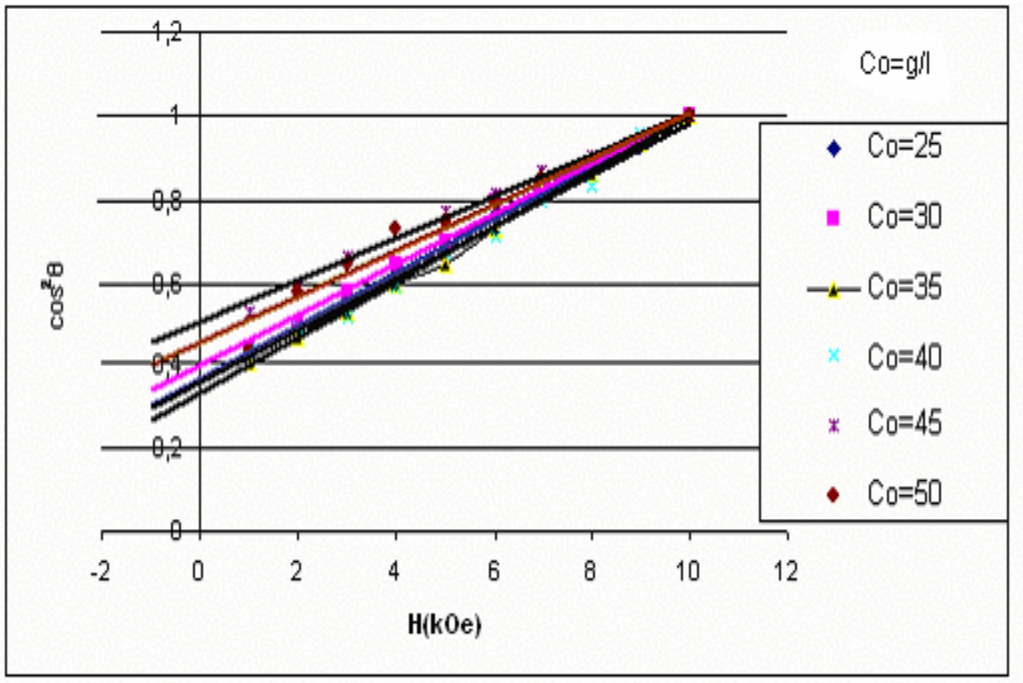

Figure 4. 13 The variation of $<\cos^2\theta>$ with the applied field.

Figure 4.13 shows the variation of $<\cos^2\Theta>$ with the applied field. At 10 kOe at which the highest magnetoresistance value is obtained, the $<\cos^2\Theta>$ value therefore gets unity. As the magnetic field decreases the angle also decreases indicating the separation of the magnetization vector from the applied field direction and reduction in magnetoresistance value. As this behavior of magnetization

develops the seperations among the $<\cos^2\Theta>$ values in the samples are observed with decreasing magnetic field. At 0kOe a maximum separation in $<\cos^2\Theta>$ is obtained. The difference of $<\cos^2\Theta>$ at 0kOe between the samples may be from the results of; i) the different unsaturation behavior of magnetization and therefore magnetoresistance effect at 10 kOe i.e. their different saturation trend with magnetic field and ii) the different non-random distribution of magnetic moments at 0 kOe in our samples.

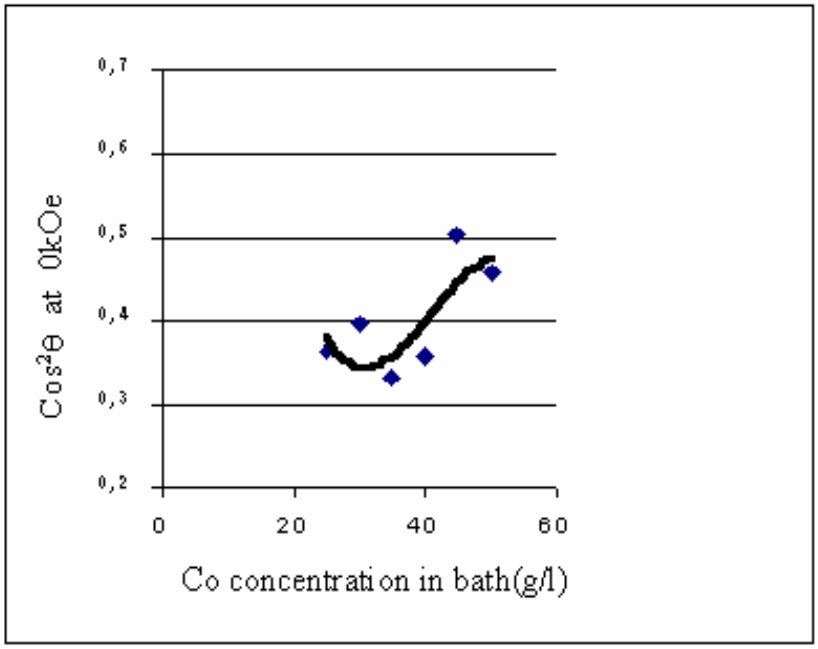

Figure 4. 14 The variation of $<\cos^2\Theta>$ at 0kOe with the Co concentration in the bath

The variation of $<\cos^2\Theta>$ at 0kOe with the Co concentration in the bath is shown in Figure 4.14. The lowest value of $<\cos^2\Theta>$ is detected in the sample with the bath Co content of 35g/l. This may indicate that the most random magnetic moment distribution and/or the fastest track which leads to quicker saturation are in this sample when compared with the other samples as the same result is seen from the MR curves in Figure 4.3.

CHAPTER 5

CONCLUSION

Magnetic multilayer and granular alloy systems are important systems for the data storage and reading heads. Several techniques are used to fabricate such magnetic systems, e.g., sputtering, evaporation, electrodeposition MBE etc. The electrodeposition technique has some advantageous over the others. It is cheaper, easier and has more controllable deposition parameters.

The giant magnetoresistance effect (GMR) is observed in the magnetic multilayer systems and magnetic granular films. Magnetic multilayer systems show high GMR properties due to the spin dependent interface scattering. Magnetic granular films exhibits relatively lower GMR effect resulted from the spin dependent scattering at magnetic grain boundaries. The Co/Cu multilayer and CuCo granular alloys are vastly investigated GMR systems as mentioned in the previous chapters.
Adding a different magnetic component, such as Ni, Fe etc, or a non-magnetic component, such as Ag, Zn etc., may affect the GMR properties of CuCo alloy systems. In this study, to see the effect of an additional non-magnetic component on the GMR properties of CuCo system and to make a comparison between the GMR values of these systems, CuAgCo systems are fabricated by electrodeposition technique. Three types of CuAgCo films were grown by varying i) Co content in bath, ii) the bath pH and iii) the deposition current density. Compositional analyses indicate that all our films are mainly composed of Cu and Co elements. The amount of silver component in each system was at most 1%. The amount of Ag component in any film did not increase even when Co and Cu contents in bath were varied, and the magnitude of Ag component persisted around 1% in all the films grown in this study. SEM studies show that the CuAgCo films have granular nature.

The magnitude of the MR value in our films varied between 0.3% and 1% for the films of the Co variation from 25g/l to 50g/l, between 0.5% and 0.9% for the films of the pH variation of 5.2 to 6 and between 0.3% and 0.8% for the films of the current variation between 2.5 and 4.5 mA/cm^2. In the longitudinal and transverse MR

measurements generally an isotropic behavior was detected. Although the isotropic behavior mainly indicates the GMR presence, a small anisotropic magnetoresistance (AMR) component was also detected in some of the films. The presence of AMR may be attributed to the coalescence of Co grains under the certain preparation conditions: Above certain threshold limits of the amount of Co component in bath, the pH value and the deposition current density, the connection of the magnetic grains may be formed. Above the 32% Co content in the film and above the bath pH value of 5.6, a decrease in MR effect and the presence of anisotropic MR effect were detected while below these values of the Co content and pH, the CuAgCo films show isotropic and increasing MR effect with increasing Co content and pH. An irregular variation of the MR effect was seen in the current variation films. From the MR curves it may therefore be deduced that below the 32% Co content and below the pH value of 5.6, the magnetic Co entities in our films form superparamagnetic grains whereas the Co grains may be connected to each other to form ferromagnetically coupled grains in these films with the Co content higher than 32% and in the films with the pH value higher than 5.6 which results in the creation of AMR.

In the analysis of our superparamagnetic CuAgCo films which have Co content less than 32% or were prepared with a pH value less than 5.6, the assumption of the superparamagnetic behavior of small magnetic Co grains was employed. From this analysis, the average magnitude of Co grain was obtained to be between 9 Å and 10Å. Any correlation between the surface to volume ratio of Co grains and the highest MR at 10kOe was not detected but a linear increase in the MR value at 10kOe with the increasing Co grain concentration was found in the CuAgCo films of Co and pH variations.

A future study may be designed to determine the electrodeposition conditions to fabricate CuAgCo granular films with more Ag component than that this study and investigate their structural and MR properties.

REFERENCES

[1] A. E.Berkowitz, J. R. Mitchell, M. J. Carey, A. P. Young, S. Zhang, F. E. Spada, F.T. Parker, A.Hutten, G. Thomas, Phys. Rev. Lett. **68,** 3745 (1992) .

[2] J. Q. Xiao, J.S.Jiang, C.L. Chien, Phys. Rev. Lett. **68,** 2472 (1992) .

[3] A. Elif Ensari, *The Characterization of Ni/Cu NanoLayers*, Uludağ University, M. Sc. Thesis Uludağ University The Graduate School of Natural and Applied Science (2004)

[4] G.Chawa, G. D. Wilcox, D. R. Gabe, Trans IMF **76,** 117 (1998) .

[5] M. R. Kalantary, G. D. Wilcox, D. R. Gabe, Br. Corrosion J. **33,** 197 (1998) .

[6] A. M. Herman, M. Mansour, V. Badri, B. Pinkhasov, C. Gonzales F. Fickett, M.E. Calixto, P. J. Sebastian, C. H. Marshall, T. J. Gillepie, Thin Solid Films **361-162,** 74 (2000) .

[7] A. A. Pasa, W. Schwarzacher, Phys. Stat. Sol. **73**, 173 (1999

[8] I. Zhitomirsky, A. Kohn, and L. Gal-or, ,*Cathodic Electrosnthesis of PZT films. Mater. Lett.* , **25** (1995).

[9] H. Konno, M. Tokita, and R. Furuchi, '*Formation of Perovskite Structure* $La_{1-x}C_xCrO_3$ *Films with Electrodeposition,'J. Electrochem.* Soc . **137** (1990).

[10] G. Zotti , '*Electrodeposition of Amorphous* Fe_2O_3 *Films by Reduction of Iron Perchlorate in Acetonitrile*, 'Electrochem. Soc.145 (1998) .

[11] P. C. Andricacos,C. Uzoh, J.O. Dukovic, J. Horskans and H. Deligianni , *Abstracts 193rd Meeting of the Electrochemical Society*, Vol. **98-1**, Abstract No . 254 .

[12] V. M. Dubin and R. Cheung, *Abstracts 193rd Meeting of the Electrochemical Society*, Vol. **98-1**, Abstract No. 242.

[13] W.Schwarzacher and D. J. Lashmore, *IEE Trans. Magnetics* **32**, 3133 (1996) .

[14] S. K. J. Lenczowski, C. Schönenberger, M. A. M. Gus, and W. J. M. DE Jonge, J. *Magn.Magn. Mater*. **148**, 455 (1995) .

[15] Feynman, RP, RB Leighton, M Sands. *The Feynman Lectures in Physics* . Addison- Wesley Publishing , Reading, Mass. U.S.A. (1977)

[16] Jiles, D. *Introduction to Magnetism and Magnetic Materials*. Chapman & Hall, ISBN 0412386402 (1991)

[17] Kip, A. *Fundamentals of Electricity and Magnetism*. McGraw-Hill, New York, U.S.A. (1962)

[18] C.P.Bean, J. *Applied Physics* **26,** 1381 (1955).

[19] All Rights Reserved J. Ray Ballinger, (1994-1996)

[20] G.Binasch, P. Grünberg, F. Saurenbach, and W. Zinn, Phys. Rev. B **39**,

[21] M. N. Baibich, J. M. Broto, A. Fert, F. Nguyen Van Dau, F. Petroff, P. Etienne, G . Creuzet , A. Friederich, and J. Chazelas, Phys. Rev. Lett. **61**, 2472(1988)

[22] T. Thio. *Metal, Phys. Rev*. B **57**, 12239 (1998)

[23] J.Q.Xiao, J.S. Jiang, C.L. Chien, *Phys.Rev*.B 46 (**14,** 9266) (1992).

[24] (M.Kuzmunski, A.Slawska-Waniewska, H.K.Lachowich, M.Knobel,J. *Magn. Mag.Mater*., **205,** 7 (1999).

[25] E.F.Ferrari, F. C. s. da Silva, M. K. *Nobel Phys.Rev*.B56 (**10,** 6086)(1997)

[26] P. Allia, M.Knobel, P.Tiberto, F. Vinai, *Phys.Rev*.B52 (**21,** 15398)(1995).

[27] R.C. O.Handley, *Modern Magnetic Materials, Principles and applications*, New York: Wiley Interscience 200; *Alignment of the disordered surface spinsunder high magnetic field* (2000).

[28] (C.Bellourad, B.George, G.Marchal, *J. Phys. : Condens Mater*.**6**, 7239(1994).

[29] (J.F. Gregg, M.Tompson, S.J.Dawson, K.Ounadjela, C.R.Staddon, J.Hamman, C. Fermon, G. Saux, K. O'Grady, *Phys.Rev.* B, **49,** 1064(1994) .

[30] M.El.Hillo, K. O'Grady, R.W. Chantrell, *J.Appl.Phys.* **76,** 6811(1994)

[31] S.Honda, M. Nawate, M. Tanaka and T. Okada, *J.Appl.Phys.* **82,** 764 (1997).

[32] R. Shull and G.C. Hadjipanayis in Shull 1998, the proceedings of the WTEC U. S. nanotechnologies workshop, 43 - 58; Hadjipanayis, (**107-112**) (1998).

[33] Abeles, B. Applied Solid State Science: *Advances in Materials and Device Research*, edited by Wolfe, R. Academic Press, New York, p. **1**, (1976).

[34] Evetts , *J. Concise Encyclopedia of Magnetic and Superconducting Materials,* Pergamon, London, p. **246**, (1992).

[35] Chartterjee , A.; Datta, A.; Giri, Anit. K . ; Das, D.; Chakravorty, *D. J. Appl. Phys*.v. 72, n. 8, p. **3832**, (1992).

[36] Wang, Jian-Ping; Luo, He-Lie; Gao, Nai-Fei; Liu, Yuan-Yuan; *J. Mater. Sci.* , v. 31, p. **727**, (1996) .

[37] Gómez, J.A.; Xia, S.K.; Passamani, E.C.; Giordanengo, B.; Baggio-Saitovitch,

E. M. J. Magn. Magn . Mater . v. 223, p. **112**, (2001).

[38] E. Budevski, G. Staikov, and W. J. Lorenz, *Electrochemical Phase Formation and Growth,* VCH, Weinheim, (1996).

[39] John Q. Xiao, J. Samuel Jiang, and C. L. Chien Department of Physics and Astronomy, The Johns Hopkins University, Baltimore, Maryland 2121
Received 5 March (1992).

[40] A.Brenner, "*Electrodeposition of alloys*", Vol. 1, Academic Pres. INC. (1963).

[41] B. Dacuna, J.Mira, M.C. Blanco, M. Lopez-Quintela, J. Rivas, *J. Mag. Mag. Mat*. **203,** 123 (1999) .

[42] M. K. Roy, P.M.G. Nambissan, H.C. Verma, *Journal of Alloys and Compounds* **1 ,** 38 (2002).

[43] S. Strehle, S. Menzel, H. Wendrock, J. Acker, K. Wetzig, Microelectronic Engineering **70** , 506 (2003).

[44] V. M. Fedosyuk, O.I. Kasyutich, W. Schwarzacher, *J. Magn. Magn. Mat.* **198**,246 (1999) .

[45] G. R. Pattanaik, D.K. Pandya, S.C. Kashyap, *J. Electrochem. Soc*. C363 . **149** (2002)

[46] M. B. Stearns and Y. Cheng, *J. Appl.Phys*. **75**, 6894 (1994) .

[47] A.N. Pohorilyi, A.F. Kravetz, E.V. Shipil, A. Ya . Vovk, Chang Sikh Kim and H.R. Khan, *J.Magn.Magn. Mat*. **87,** 186 (1998) .

[48] Y. Asona, A. Oguri, *J. Inoue and S.Maekawa Physical Review B* **49,** 12831 (1994).

[49] S. Ge, H. Li, C.Li, Li Xi, W. Li and J. Chi, *J. Phys. : Condens. Mater* . **12**, 5905 (2000).

[50] B.D.Cullity, *Introduction to Magnetic Materials*, Addison-Wesley Pres, (1972)